

**STUDIES ON VARIATION OF BOUNDARY LAYER
PARAMETERS ON ROUGH SURFACES IN
TURBULENT BOUNDARY LAYER ZONE**

*A Thesis Submitted in Partial Fulfillment of the Requirements
for the Degree of*

**MASTERS OF TECHNOLOGY
IN
CIVIL ENGINEERING**



**BY
ARUNIMA SINGH**

**DEPARTMENT OF CIVIL ENGINEERING
NATIONAL INSTITUTE OF TECHNOLOGY, ROURKELA
2013-15**

STUDIES ON VARIATION OF BOUNDARY LAYER PARAMETERS ON ROUGH SURFACES IN TURBULENT BOUNDARY LAYER ZONE

*A Thesis Submitted in Partial Fulfillment of the Requirements
for the Degree of*

*Master of Technology
In
Civil Engineering*

WITH SPECIALIZATION IN

WATER RESOURCES ENGINEERING

Under the guidance and supervision of

Prof Awadhesh Kumar

Submitted By:

ARUNIMA SINGH

(ROLL NO. 213CE4113)



**DEPARTMENT OF CIVIL ENGINEERING
NATIONAL INSTITUTE OF TECHNOLOGY, ROURKELA
2015**



**National Institute of Technology
Rourkela**

CERTIFICATE

This is to certify that the thesis entitled “**STUDIES ON BOUNDARY LAYER PARAMETERS ON ROUGH SURFACES IN TURBULENT BOUNDARY LAYER ZONE**” being submitted by **ARUNIMA SINGH** in partial fulfillment of the requirements for the award of *Master of Technology* Degree in *Civil Engineering* with specialization in *Water Resources Engineering* at National Institute of Technology Rourkela, is an authentic work carried out by her under my guidance and supervision.

To the best of my knowledge, the matter embodied in this report has not been submitted to any other university/institute for the award of any degree or diploma.

Dr. Awadhesh Kumar

Water Resources Engineering

Department of Civil Engineering

Place: Rourkela

Date:

ACKNOWLEDGEMENT

A complete research work can never be the work of anyone alone. The contributions of many different people, in their different ways, have made this possible. One page can never suffice to express the sense of gratitude to those whose guidance and assistance was indispensable for the completion of this project.

I would like to express my special appreciation and thanks to my supervisor Professor Dr. Awadhesh Kumar you have been tremendous mentor for me. I would like to thank you for encouraging my research and for allowing me to grow as a research scholar. Your advices on both researches as well as on my career have been priceless.

I would also like to thank my committee members, Professor, Sishir Sahu; Head of the Civil Department. And also I am sincerely thankful to Prof. K.C. Patra, and Prof. K.K.K. Khatua for their kind cooperation and necessary advice. I also want to thank you for letting my seminars be an enjoyable moment, and for your brilliant comments and suggestions, thanks to you.

I wish to express my sincere gratitude to Dr. S K Sarangi, Director, NIT, Rourkela for giving me the opportunities and facilities to carry out my research work.

A special words of thanks to Ms. Monalisa Mallick, Mr Arpan Pradhan and Mr. Abinash Mohanta Ph.D. scholar of Civil Engineering Department, for their

suggestions, comments and entire support throughout the project work. I express my special thanks to my dear friends Deepika, Anta, Saudamini, Rajendra, for their continuous support, suggestions and love.

Last but not least I would like to thanks to my father Mr. Niranjan Singh and mother Mrs. Nibedita Singh, who taught me the value of hard work by their own example. Thanks a lot for your understanding and constant support, and to my sister Arpita Singh, brother Abhijeet Kumar Rout and uncle Mr. Ananta Bai for his encouragement. They rendered me enormous support during the whole tenure of my study at NIT Rourkela. Words cannot express how grateful I am to my Father, Mother, Sister, Brother, Uncle for all of the sacrifices that you have made on my behalf. Your prayer for me was that sustained me thus far.

Arunima Singh

ABSTRACT

At the point when genuine fluid streams past a solid body or a solid boundary wall, the fluid particles adhere to the wall and state of no slip happens. This implies that the velocity of fluid near to the wall will be same as that of wall. On the off chance that the wall is stationary, the speed of fluid at the boundary will be zero. Further far from the limit, the velocity will be higher and as a consequence of this variety of velocity, and gradient of velocity will exist. The speed of fluid increments from zero on the stationary limit to the free stream velocity of the fluid in the direction normal to the boundary. This velocity from zero to free stream velocity in the perpendicular direction to the wall happens in a restricted locale in the region of solid boundary. This narrow locale of fluid is called Boundary Layer.

Three fundamental parameters (portrayed underneath) that are utilized to describe the size and state of a boundary layer are the nominal boundary layer thickness, the displacement thickness, and the momentum thickness. In our proposition, we have gotten the boundary layer parameters and velocity profiles on different types of rough surfaces by using wind tunnel. The emery papers of distinctive grain sizes have been considered as rough surfaces.

This paper summarizes a select set of recent investigations involving the computations of effects of roughness, mainstream velocity and distance from leading edge on turbulent boundary layer along with the correlations.

Keywords: *Surface Roughness, Velocity Profile, Boundary layer, Turbulent Flow, Correlation, Wind Tunnel.*

TABLE OF CONTENTS

<u>CONTENTS</u>	<u>PAGE</u>
CERTIFICATE	I
ACKNOWLEDGEMENT	II
ABSTRACT	IV
TABLE OF CONTENTS	V
LIST OF FIGURES	VIII
LIST OF TABLES	XI
TABLE OF NOMENCLATURE	XII
CHAPTER 1	
<i>INTRODUCTION</i>	1
1.1 WIND AND TURBULENCE	1
1.2 BOUNDARY LAYER THEORY	2
1.3 TURBULENT BOUNDARY LAYER	3
1.4 BOUNDARY LAYER PARAMETERS	3
1.4.1 Boundary layer thickness	3
1.4.2 Displacement thickness	3
1.4.3 Momentum thickness	4
1.4.4 Energy thickness	4
1.4.5 Drag & Lift forces	4
1.4.6 Surface Shear Stress	5
1.5 SURFACE ROUGHNESS	5
1.6. ABOUT WIND TUNNEL	5
1.6.1. What Are Wind Tunnels	5
1.6.2 Flow Classification	6
1.6.3. How Do Wind Tunnels Work	8
1.7. ORGANISATION OF THESIS	8
CHAPTER 2	
<i>OBJECTIVES AND SCOPE</i>	10

CHAPTER 3	
<i>LITERATURE REVIEW</i>	11
3.1. GENERAL	11
CHAPTER 4	
<i>EXPERIMENTATION</i>	16
4.1. GENERAL	16
4.2. WIND TUNNEL USED IN THE EXPERIMENT	16
4.3 EQUIPMENTS	18
4.3.1. Digital velocity meter	18
4.3.2. Telescopic pitot-tube	19
4.3.3. Rough flat plates	19
4.3.4. Special trolley arrangement	21
4.3.5. Tachometer	22
4.4 SET-UP	22
CHAPTER 5	
<i>METHODOLOGY</i>	24
CHAPTER 6	
<i>RESULTS AND DISCUSSION</i>	25
6.1. OVERVIEW	25
6.2 VELOCITY PROFILES	25
6.3 VELOCITY VARIATIONS AT A PARTICULAR SECTION AND ROUGHNESS FOR CHANGING MAIN STREAM VELOCITY	32
6.4 VELOCITY VARIATIONS AT A PARTICULAR SECTION AND FREE STREAM VELOCITY FOR CHANGING ROUGHNESS	35
6.5. BOUNDARY LAYER GROWTH	36
6.5.1. Boundary layer variations at constant free stream velocity for varying roughness	36
6.5.2. Boundary layer variations at constant roughness for varying free-stream velocities	38
6.6. CALCULATIONS OF PARAMETERS	40
6.6.1. Determination of boundary layer parameters	41

6.7. DISCUSSION	48
CHAPTER 7	
<i>DEVELOPMENT OF CORRELATION</i>	50
7.1 GENERAL	50
7.2. DATA PROCESSING	50
7.3. CORRELATION PLOTS FOR ALL THE BOUNDARY LAYER PARAMETERS	60
7.4. CORRELATION ESTABLISHMENT	66
7.5. COMPARISON GRAPHS OF BOUNDARY LAYER PARAMETERS	67
7.6. CONCLUSIONS	69
7.7. SCOPES FOR FUTURE WORK	70
<i>REFERENCES</i>	71
<i>PUBLICATIONS FROM WORK</i>	72

FIG. NO.	LIST OF FIGURES	PAGE
1.1	Laminar and Turbulent behavior of fluid	2
1.2	Parts of a typical wind tunnel	8
4.2.1	Wind tunnel used for the Project	17
4.2.2	Driving unit of wind tunnel	18
4.3.1	Digital velocity-meter	19
4.3.2	Telescopic Pitot-Tube	19
4.3.3(a)	Rough surfaces of Grade 40 and 50	20
4.3.3(b)	Rough surfaces of Grade 60 and 120	20
4.3.4	Special Trolley Arrangement	21
4.3.5	Digital Laser Tachometer	22
4.4	Test section of Experiment	23
6.2.1	Velocity profiles at various sections for $k=375\mu\text{m}$ and $V=10.9\text{m/s}$	25
6.2.2	Velocity profiles at various sections for $k=375\mu\text{m}$ and $V=12.5\text{m/s}$	26
6.2.3	Velocity profiles at various sections for $k=375\mu\text{m}$ and $V=13.6\text{m/s}$	26
6.2.4	Velocity profiles at various sections for $k=345\mu\text{m}$ and $V=10.9\text{m/s}$	27
6.2.5	Velocity profiles at various sections for $k=345\mu\text{m}$ and $V=12.5\text{m/s}$	27
6.2.6	Velocity profiles at various sections for $k=345\mu\text{m}$ and $V=13.6\text{m/s}$	28
6.2.7	Velocity profiles at various sections for $k=290\mu\text{m}$ and $V=10.9\text{m/s}$	28
6.2.8	Velocity profiles at various sections for $k=290\mu\text{m}$ and $V=12.5\text{m/s}$	29
6.2.9	Velocity profiles at various sections for $k=290\mu\text{m}$ and $V=13.6\text{m/s}$	29
6.2.10	Velocity profiles at various sections for $k=125\mu\text{m}$ and $V=10.9\text{m/s}$	30

6.2.11	Velocity profiles at various sections for $k=125\mu\text{m}$ and $V=12.5\text{m/s}$	30
6.2.12	Velocity profiles at various sections for $k=125\mu\text{m}$ and $V=13.6\text{m/s}$	31
6.3.1	Velocity Profiles At section $x=70\text{cm}$ for varying Main-stream velocities	32
6.3.2	Velocity Profiles At section $x=80\text{cm}$ for varying Main-stream velocities	33
6.3.3	Velocity Profiles At section $x=90\text{cm}$ for varying Main-stream velocities	34
6.4.1	Velocity Variations At $x=70\text{cm}$ for varying free-stream velocities	35
6.4.2	Velocity Variations At $x=80\text{cm}$ for varying free-stream velocities	35
6.5.1(a)	Boundary layer growth in Turbulent B/L zone for $V=10.9\text{m/s}$	36
6.5.1(b)	Boundary layer growth in Turbulent B/L zone for $V=12.5\text{m/s}$	37
6.5.1(c)	Boundary layer growth in Turbulent B/L zone for $V=13.6\text{m/s}$	37
6.5.2(a)	Boundary layer growth in Turbulent B/L zone for $k=375\mu\text{m}$	38
6.5.2(b)	Boundary layer growth in Turbulent B/L zone for $k=345\mu\text{m}$	38
6.5.2(c)	Boundary layer growth in Turbulent B/L zone for $k=290\mu\text{m}$	39
6.5.2(d)	Boundary layer growth in Turbulent B/L zone for $k=125\mu\text{m}$	39
6.7.1(a)	For $\frac{y}{\delta}$ vs. $\frac{\vartheta}{V}$ at $V=10.9\text{m/s}$, $x=85\text{cm}$ and $k=375\mu\text{m}$	41
6.7.1(b)	For $\frac{y}{\delta}$ vs. $\frac{\vartheta}{V}$ at $V=10.9\text{m/s}$, $x=85\text{cm}$ and $k=345\mu\text{m}$	43
6.7.1(c)	For $\frac{y}{\delta}$ vs. $\frac{\vartheta}{V}$ at $V=10.9\text{m/s}$, $x=85\text{cm}$ and $k=290\mu\text{m}$	43
6.7.1(d)	For $\frac{y}{\delta}$ vs. $\frac{\vartheta}{V}$ at $V=10.9\text{m/s}$, $x=85\text{cm}$ and $k=125\mu\text{m}$	44
6.7.1(e)	For $\frac{y}{\delta}$ vs. $\frac{\vartheta}{V}$ at $k=375\mu\text{m}$, $x=85\text{cm}$ and $V=12.5\text{m/s}$	45
6.7.1(f)	For $\frac{y}{\delta}$ vs. $\frac{\vartheta}{V}$ at $k=375\mu\text{m}$, $x=85\text{cm}$ and $V=13.6\text{m/s}$	46
6.7.1(g)	For $\frac{y}{\delta}$ vs. $\frac{\vartheta}{V}$ at $k=375\mu\text{m}$, $V=10.9\text{m/s}$ and $x=90\text{cm}$	46
6.7.1(h)	For $\frac{y}{\delta}$ vs. $\frac{\vartheta}{V}$ at $k=375\mu\text{m}$, $V=10.9\text{m/s}$ and $x=95\text{cm}$	47
7.2.1	Determination of n_1 For Nominal/Boundary layer Thickness	52
7.2.2	Determination of n_2 For Nominal/Boundary layer Thickness	53

7.2.3	Determination of n_3 For Nominal/Boundary layer Thickness	53
7.2.4	Determination of n_1 For Displacement Thickness	54
7.2.5	Determination of n_2 For Displacement Thickness	54
7.2.6	Determination of n_3 For Displacement Thickness	55
7.2.7	Determination of n_1 For Momentum Thickness	55
7.2.8	Determination of n_2 For Momentum Thickness	56
7.2.9	Determination of n_3 For Momentum Thickness	56
7.2.10	Determination of n_1 For Energy Thickness	57
7.2.11	Determination of n_2 For Energy Thickness	57
7.2.12	Determination of n_3 For Energy Thickness	58
7.3.1	Correlation Plot of Nominal Thickness with System Variable	60
7.3.2	Correlation Plot of Displacement Thickness with System Variable	60
7.3.3	Correlation Plot of Momentum Thickness with System Variable	63
7.3.4	Correlation Plot of Energy Thickness with System Variable	63
7.4.1	Comparison between experimental and predicted values of Nominal B/L Thickness (δ)	67
7.4.2	Comparison between experimental and predicted values of Displacement Thickness (δ^*)	67
7.4.3	Comparison between experimental and predicted values of Momentum Thickness (θ)	68
7.4.4	Comparison between experimental and predicted values of Energy Thickness (δ_E)	68

Table No.	LIST OF TABLES	Pages
1.6	Range of Mach No.	7
4.2.1	Specification of Laboratory Wind Tunnel Components	17
4.3.1	Dimensions of Flat Plate Surface	21
4.3.2	Roughness height	21
6.7.1	Calculated values of Boundary Layer Parameters with system Variables	49
7.2.1	Exponents obtained from the Equations	59
7.3.1	Comparison of Experimental and Predicted values of Nominal B/L Thickness using Developed Correlation	61
7.3.2	Comparison of Experimental and Predicted values of Displacement Thickness using Developed Correlation	62
7.3.3	Comparison of Experimental and Predicted values of Momentum Thickness using Developed Correlation	64
7.3.4	Comparison of Experimental and Predicted values of Energy Thickness using Developed Correlation	65

TABLE OF NOMENCLATURE	
τ	Surface Shear Stress
μ	Co-efficient of Dynamic Viscosity
ν	Kinematic viscosity
$\frac{dv}{dy}$	Velocity Gradient
H	Shape Factor
L	Length
M	Mach Number
Re	Reynolds Number
C_d	Drag Co-efficient
v	Velocity at a particular position
V	Main stream velocity
y	Height of a point from the flat surface
x	Distance from the Leading edge
k	Height of Roughness
δ	Boundary Layer Thickness
δ^*	Displacement Thickness
θ	Momentum Thickness
δ_E	Energy Thickness
R^2	Regression Co-efficient
C	Constant Correlation Coefficient
f	Function
BND	Bivariate Normal distribution
DNS	Direct Numerical Simulation
DPIV	Digital Particle Image Velocimetry
CFD	Computational Fluid Dynamics
ZPG	Zero Pressure Gradient



1. INTRODUCTION

1.1. WIND AND TURBULENCE

Wind and turbulence is experienced in regular life. It influences how planes fly, the proficiency of vehicles travel and our capability to the foresee climate and atmosphere. Moving air is wind. Wind has speed rate and directions. The momentary wind speed is involved 3 parts, the mean wind speed, an occasional or periodic velocity of wave and irregular fluctuating speeds. The mean wind advects material. Waves have a tendency to happen around evening time under stable warm stratification. In the event that they are general they transport almost no warmth and mass. Fluctuating part of wind is connected with turbulence. This segment is vital on the grounds that it is a system for transporting heat, energy and mass between the biosphere and atmosphere. The investigation of fluid stream is complex. It contains movements that are highly composed (like a Whirl-wind, tornado or typhoon) and riotous (as in turbulent flow). The investigation of fluid stream and turbulence is considered by numerous to stay one of the unsolved issues of present day material science or physics.

The famous fluid mechanic, Theodore von Karman, is credited with stating:

‘There are two great unexplained mysteries in our understanding of the universe. One is the nature of a unified generalized theory to explain both gravity and electromagnetism. The other is an understanding of the nature of turbulence. After I die, I expect God to clarify the general field theory to me. I have no such hope for turbulence’.

Turbulence is the disorganized and apparently arbitrary movement of liquid packages. Turbulence has origin of mechanical and convective mechanisms. Shear cause mechanical turbulence while unstable buoyant forces (because of the mixing of fluid bundles with diverse densities) cause convective turbulence. Barometrical turbulence varies from turbulence produced in a research facility or in funnel/pipe stream. In the air, convective turbulence with mechanical turbulence, co-exist.

Turbulent flow has a number of unique properties. Turbulence is a complex phenomenon defined by the tumultuous and apparently arbitrary movement of fluid packages, on one hand, and coherent elements on the other. On a fundamental level, turbulence is: 1) Non-linear, 2) Non-Gaussian, 3) Three dimensional, 4) Diffusive, 5) Dissipative, and 6) contains a range of length scale.

1.2 BOUNDARY LAYER THEORY:

The theory of boundary layer flow of fluids plays the leading part of modern fluid dynamics especially for the low viscous fluids like air and water. The concept of boundary layer theory was introduced by Ludwig Prandtl, who conceived and had given the idea of a layer characteristic of fluids in the region of a solid boundary. He proposed that even for a very small viscosity of a viscous fluid the no slip condition must be satisfied at the solid boundary. No slip condition implies that the velocity of the fluid at a solid boundary is same as that of the boundary itself.

The boundary layer exists in the real fluid flow past a solid boundary. For example flow of water in an open channel, in a pipe, air flow within a wind tunnel etc. wherever the flowing fluid contacts with any kind of solid boundary vicinity there exist a boundary layer.

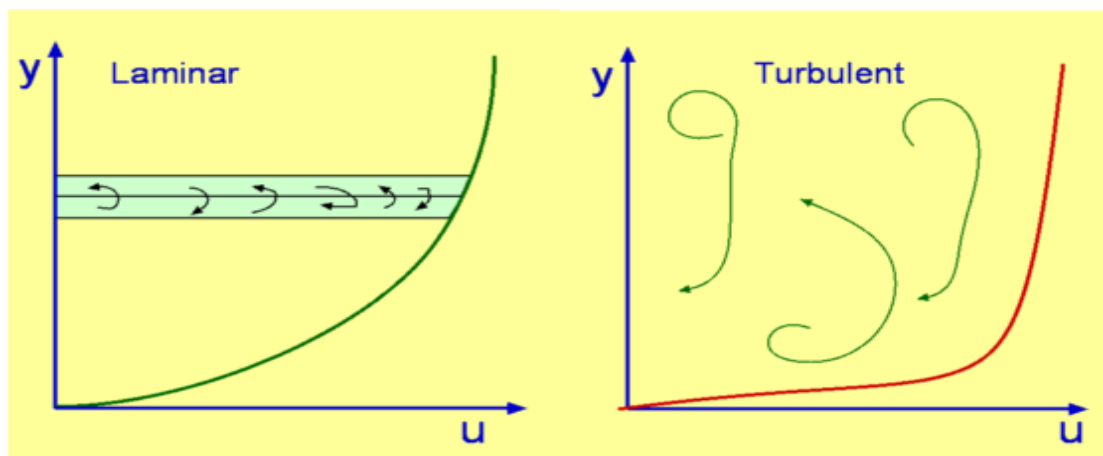


Fig. No.1.1, Laminar and Turbulent behaviour of fluid



1.3 TURBULENT BOUNDARY LAYER:

In turbulent flow, the boundary layer is defined as the region of a thin layer on the surface of a body in which viscous effects are important. The boundary layer permits the fluid to transition from the free stream velocity (V) to a velocity of zero at the wall. The viscous fluid flow over a solid surface encounters frictional forces, which retard the motion of the fluid in a thin layer close to the wall. The development of the layer is a major contributor to flow resistance on streamlined geometries and is of great importance in many engineering problems. The concept of a boundary layer is largely due to Prandtl in 1904, as reported by White (1974). He showed that the friction effects inside the fluid are significant only in a slender layer near to the surface. Many important applications has to deal with the use of boundary layer theory, such as the computation of flow separation and skin friction drag.

1.4 BOUNDARY LAYER PARAMETERS:

The important parameters used to analyze the shape and size of any boundary layer are, the boundary layer thickness, displacement thickness, momentum thickness and energy thickness. The shape of the boundary layer is described by ratios of these thicknesses.

1.4.1. Boundary layer thickness- The distance measured normal to a boundary layer from the wall or boundary, to a point where the flow velocity occupy the free stream velocity (V), is termed as boundary layer thickness δ . Basically the point where the flow velocity is that of the free stream is usually characterized as the point where:

$$\delta = 0.99V$$

1.4.2. Displacement thickness- The distance by which a surface would have to be displaced in the direction normal to its normal vector away from the plane of reference in an inviscid fluid in motion, of velocity V to give the same rate of flow as takes place between the reference plane and the surface, in a real fluid.

The displacement thickness can be calculated by,

$$\delta^* = \int_0^{\delta} \left(1 - \frac{v}{V}\right) dy$$



INTRODUCTION

The boundary layer's shape factor is calculated by the displacement thickness.

A shape factor is used to determine the nature of the flow in boundary layer flow.

$$H = \frac{\delta^*}{\theta}$$

For value of H, stronger will be the adverse pressure gradient. The Reynolds number can be reduced by a high adverse pressure gradient at which transition into turbulence may occur.

1.4.3. Momentum thickness- The distance by which a surface is to be moved parallel to itself towards the plane of reference in an inviscid fluid of velocity V giving the existence of same total momentum to compensate for the deficit of momentum loss between the reference plane and the surface, in the fluid is the momentum thickness (θ).

The momentum thickness can be calculated by,

$$\theta = \int_0^{\delta} \frac{v}{V} \left(1 - \frac{v}{V}\right) dy$$

1.4.4. Energy thickness- The distance normal to the boundary of the solid body, by which the boundary should be displaced in such way for the compensation of the depletion in kinetic energy of the fluid flow on the behalf of boundary layer formation is the energy thickness, δ_E .

The energy thickness can be determined by,

$$\delta_E = \int_0^{\delta} \frac{v}{V} \left[1 - \left(\frac{v}{V}\right)^2\right] dy$$

1.4.5. Drag & Lift forces- The surrounding fluid imparts pressure and viscous forces on a submerged object. The components of the resultant force acting on the immersed object in the fluid are the drag force and the lift force. The friction drag (or viscous drag) is produced by the shear stresses acting tangentially on the object. Pressure or form drag results from variations in the normal pressure around the object.

The drag force acts in the direction of the motion of the fluid relative to the object.

The lift force is normal to the flow direction.



INTRODUCTION

Both are influenced by the size and shape of the object and the Reynolds number of the flow.

1.4.6. Surface Shear Stress- In the boundary layer region, the velocity gradient $\frac{du}{dy}$ exists. Hence the fluid exerts a shear stress on the wall in the direction of motion. The value of shear stress is given by,

$$\tau = \mu \frac{du}{dy}$$

1.5 SURFACE ROUGHNESS:

A component of surface texture is Roughness (k). The vertical deviations of a real surface from its ideal form defines the surface roughness. The roughness parameters are calculated by given formulae with a description to the surface. Still a standard reference describing each in detail is Surfaces and their Measurement. Roughness is often closely related to the wear properties and friction of a surface.

Many industrial applications use surface roughness information to ensure proper function of their products. Fast and accurate monitoring and measurement and measurement of surface roughness is crucial to safeguard product quality of automotive applications such as friction plates, or sealing shafts, brake shoes and pads.

1.6. ABOUT WIND TUNNEL:

1.6.1. What Are Wind Tunnels?

A wind tunnel is a specially designed machine, into which air is drawn, by mechanical means, in the purpose of achieving a specified speed and predetermined flow pattern at a given instant. From outside the wind tunnel, the flow so achieved can be observed through transparent windows enclosing the test section and flow characteristics are measurable using specialized equipments. An object can be, such as a full-size aircraft or spacecraft, a smaller-scale model of a vehicle or a part of it, or even a common object like a tennis ball, any model, or some full-scale engineering structure, which



INTRODUCTION

can be immersed into the flow established, thereby disturbing it. The objectives of the immersion include being able to observe, simulate, visualize, and measure how the immersed object is affected by the flow around it.

1.6.2. Flow Classification

There are several ways to classify wind tunnels. I have classified different types of wind tunnels and discussed some of the unique features of each type of tunnel in this section of the project. Wind tunnels can be classified as per four different criteria.

Type 1 classification –

The criterion for classification is the path followed by the drawn air.

Open-circuit (open-return) wind tunnel- The wind tunnel is said to have an open-air circuit when the air is drawn directly from the surroundings into the wind tunnel and rejected back into the surroundings. An open-circuit wind tunnel is also called an open-return wind tunnel.

Closed-circuit, or closed-return, wind tunnel- The wind tunnel is said to have a closed-air circuit, when the same air is being circulated in such a way that the wind tunnel does neither draw new air from the surrounding, nor return it into the surroundings.

Type 2 classification –

The maximum speed achieved by the wind tunnel is the criterion for classification.

The use of the ratio of the speed of the fluid, or of any other object, and the speed of sound is the traditional one. That ratio is called the Mach number. The classification is summarized in Table 1.1

Subsonic wind tunnels- If the maximum speed achieved by the wind tunnel is less than the speed of sound in air, it is called a subsonic wind tunnel. The speed of sound in air at room temperature is approximately 343 m/s, or 1235 km/hr, or 767 mile/hr.

The Mach number, $M < 1$.



INTRODUCTION

Supersonic wind tunnels- If the maximum speed achieved by the wind tunnel is equal to or greater than the speed of sound in air, it is called a supersonic wind tunnel.

Table No. 1.6

Range of Mach No. (M)	Name of Flow or Conditions
$M < 1$	Subsonic
$M = 1$, or near to 1	Transonic
$1 < M < 3$	Supersonic
$3 < M < 5$	High Supersonic
$M > 5$	Hypersonic
$M \gg 5$	High Hypersonic

Type 3 classification –

The criterion of classification is the purpose for which the wind tunnel is designed.

If the wind tunnel is for research it is called a *research wind tunnel*.

If however, it is designed to be used for education, then, it is known as an *educational wind tunnel*.

Type 4 classification –

The criterion for classification is the nature of the flow.

Boundary layer wind tunnels are used to simulate turbulent flow near and around man-made engineering structures.

1.6.3. How Do Wind Tunnels Work?

Wind tunnels usually have powerful fans to move the air through the tube. The object being tested is placed in the tunnel so that it will not move. The air moving around the still object shows what would happen if the object were moving through the air.

Usually, the object carries special instruments to measure the forces produced by the air on the object. Engineers also study how the air moves around the object by injecting smoke or dye into the tunnel and photographing its motion around the object. Improving the flow of air around an object can increase its lift and decrease its drag.

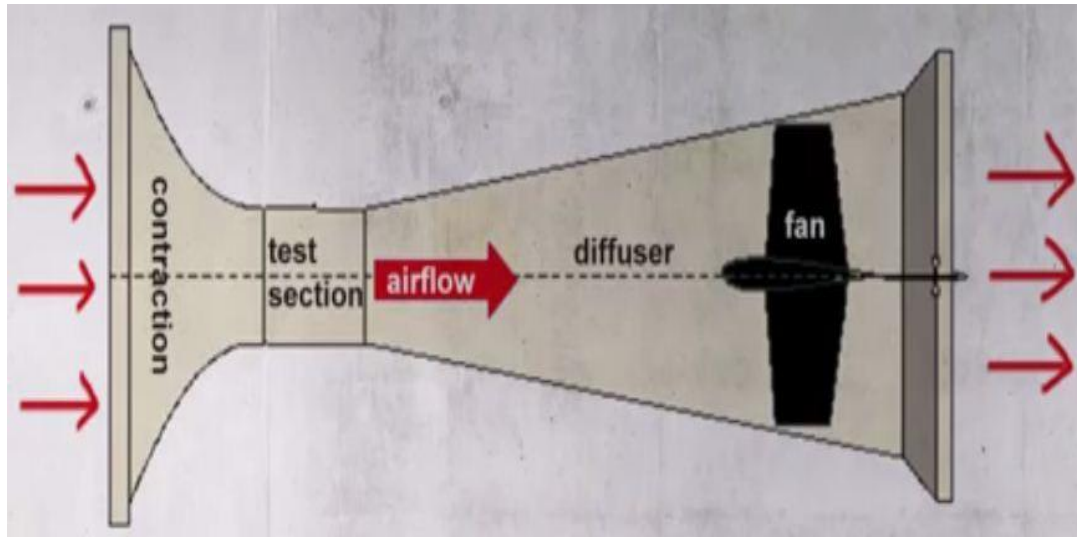


Fig. No. 1.2, Parts of a typical Wind tunnel

1.7. ORGANISATION OF THESIS:

The thesis consists of eight chapters. General *introduction* is given in Chapter 1, objectives are presented in Chapter 2, literature survey is described in Chapter 3, experimentation is explained in Chapter 4, methodology is described in Chapter 5, Chapter 6 comprises experimental results, development of correlations and conclusions are presented in Chapter 7 and finally the *references* are given in Chapter 8.



INTRODUCTION

General view on turbulence, boundary layer parameters is provided at a glance in the first chapter. Also the chapter introduces flow classifications and gives the general idea of wind tunnels.

Chapter 2 focuses on the objectives and scopes of this project work. A brief idea upon the works carried out are outlined for better understanding of the chosen topic.

Chapter 3 contains the detailed literature survey by many renowned researchers that relates partially or mostly to the present work from the beginning till date. The chapter emphasizes on the research carried out on velocity distribution on rough surfaces, the turbulence zone effects on structures, and many more complex problems regarding the works done in this field.

The laboratory setup and whole experimental procedure is clearly described in Chapter 4. This section explains the experimental arrangements and procedure adopted to obtain observation at different points of several sections above the flat plate of different roughness values. Also the detailed information about the instrument used for taking observation and geometry of experimental set up is described in this chapter.

Chapter 5 presents the methodology; which include the detailed procedure of the experiment carried out during the experimentation.

Chapter 6 gives the explanations of results of the experiment. Here typical plots are shown to compare and analyze the variations and similarities of velocity profiles and behaviors with respect to the boundary layer parameters. Calculated values of the parameters are tabulated for further analysis.

In Chapter 7, required plots are shown to enumerate the derived correlations. And also the conclusion reached by the present research.

Lastly in Chapter 8, References that have been made in subsequent chapters are provided at the end of the thesis.



2. OBJECTIVES AND SCOPE

The present work is aimed to study the effects of roughness, velocity, and longitudinal distances on the boundary layer and the boundary layer parameters over a flat plate surface for zero angle of incidence.

The objectives of the present work are summarized as:

- To measure experimentally laminar and turbulent boundary layers over a thin flat plate at zero angle of incidence inside wind tunnel.
- To study the variations of velocity profiles, boundary layer growth and other boundary layer parameters with respect to different rough surfaces and free stream velocity.
- To study the influences of surface roughness on boundary layer parameters especially in turbulence zone.
- To obtain boundary layer thickness, displacement, momentum & energy thicknesses and shear drag using velocity profiles in different cases and positions.
- Establishment of co-relation for boundary layer thickness, displacement, momentum & energy thicknesses as a function of main stream velocity, roughness parameter & positions.



3. LITERATURE REVIEW

3.1. GENERAL

Though the literature occupies an extensive variety of theories, this review will focus on theories which develop constantly. The past research works related to proposed study is described in this chapter. The researchers have made a continuous effort to study the boundary layer theory and effects on the boundary layer parameters on different bodies. The widespread use of boundary layer phenomenon has encouraged many researchers for the study of various characteristics of their flow parameters. The boundary layer parameters are influenced by many factors particularly, the distances from leading edge, the size of the roughness used and fluid velocity. It is quite essential to take into account of the velocity distribution that exists in fluid-dynamics to understand the explained characteristics and plots. So the present literature review includes works on experimental research of velocity distribution, boundary layer theory, effects of rough bodies on flow parameters in aerodynamics.

K. V. S. Namboodiri, et.al (2014) discussed the features of wind, turbulence, and surface roughness parameter over the coastal boundary layer of the Peninsular Indian Station, Thumba Equatorial Rocket Launching Station (TERLS). Every 5 min measurements from an ultrasonic anemometer at 3.3 m agl from May 2007 to December 2012 are used for this work. Symmetries in mesoscale turbulence, stress off-wind angle computations, structure of scalar wind, resultant wind direction, momentum flux (M), Obukhov length (L), frictional velocity (u^*), w -component, turbulent heat flux (H), drag coefficient (C_d), turbulent intensities, standard deviation of wind directions ($\sigma\Theta$), wind steadiness factor- relationship, bi-variate normal distribution (BND) wind model, surface roughness parameter (z_0), and wind direction (Θ) relationship, and variation of with the Indian South West monsoon activity were discussed.



LITERATURE REVIEW

James Cardillo, et.al (2013) had shown first, the direct numerical simulation (DNS) of a turbulent boundary layer at ($Re_{\theta} = 2077-2439$), performed on a rough surface with a zero pressure gradient (ZPG). The boundary layer was subjected to transitional, 24-grit sandpaper- surface roughness.

Guillermo Araya, et.al (2011) narrated the computational method involves a synergy of the dynamic multi-scale approach devised, for prescribing inlet turbulent boundary conditions and a new methodology for mapping high-resolution topographical surface data into a computational fluid dynamics (CFD) environment. The dynamic multi-scale approach can be successfully extended to simulations which incorporate surface roughness.

G.R. Spedding, et.al (2009) had carried out a series of experiments which reported, DPIV sampling parameters are driven beyond their normal range in an attempt to measure turbulence levels in a low turbulence wind tunnel.

L. C. Johansson (2009) mentioned the Digital Particle Image Velocimetry (DPIV) methods cannot easily be used to measure wind tunnel turbulence because of the low measured bandwidth.

The results show that DPIV can measure the background turbulence, and therefore its instantaneous structure. The measurements also reveal certain challenges in investigating the aerodynamic performance of small-scale flying devices.

Cheryl Klipp (U.S. Army Research Laboratory, Adelphi, Maryland) (2007) examined a variety of atmospheric boundary layer parameters as a function of wind direction in both urban and sub-urban settings in Oklahoma City, derived from measurements during the Joint Urban 2003 field campaign. He observed;

Heterogeneous surface characteristics result, significant differences in upwind fetch and, therefore, statistically significant differences in measured values, even for small changes in wind direction.



LITERATURE REVIEW

Taller upwind obstructions yield larger measured values of drag coefficient and turbulence intensity than do shorter upwind obstructions regardless of whether the obstruction is a building or a tree.

Shuyang Cao, et.al, (2006) had done wind tunnel experiments to study the effects of surface roughness on the turbulent boundary layer flow over a two-dimensional steep hill, accompanied by a relatively steady and large separation, sometimes called a separation bubble. Here he had shown;

Vertical profiles of the turbulence statistics over the hill were investigated, and compared with those for an oncoming turbulent boundary layer over a flat surface covered by cubes with the same arrangement.

Furthermore, measurements of the turbulent boundary layer flow over a smooth hill of the same shape were taken in order to identify the surface roughness effects. The speed-up ratio above the crest and the turbulence statistics in the wake were focused on.

Flow structures in the separation bubble were investigated by measuring the velocity with a split-fiber probe. Measurement with fine resolution in the streamwise direction for near-ground flows was carried out to detect the reattachment point. In addition, variations of power spectrum of longitudinal velocity fluctuation downstream of the hill are shown for surface conditions.

Carolyn D. Aubertine, et.al, (2004) examined experimentally the effects of wall roughness for two different rough-wall cases involving flow over a ramp with separation and reattachment. For these cases, the roughness Reynolds number was matched at two different momentum thicknesses Reynolds numbers. Both flow conditions were fully rough. Some of the observations are high lightened here;

The effect of increasing the wall roughness was to increase the friction velocity and increase the separation region size. The two rough-wall cases produced different size separation regions and friction velocity values. This shows that the roughness



LITERATURE REVIEW

Reynolds number is not sufficient to characterize the roughness effects. Another parameter such as the ratio of the roughness height to the boundary layer thickness is also necessary. In both cases, the outer layer turbulence was mainly affected by the change in the friction velocity.

R. A. Antonia, P-A. Krogstad (2000) shown the classical treatment of rough wall turbulent boundary layers consists in determining the effect the roughness has, on the mean velocity profile. This effect is usually described in terms of the roughness function. The general implication is that different roughness geometries with the same roughness function will have similar turbulence characteristics, at least at a sufficient distance from the roughness elements. And he concluded the Reynolds stress anisotropy is largest for a smooth wall. The small-scale anisotropy and intermittency exhibit much smaller differences when the Taylor micro-scale Reynolds number and the Kolmogorov-normalized mean shear are nominally the same.

Stefan Emeis (1990) had observed Pressure drag of obstacles in the atmospheric boundary layer was computed with a mesoscale numerical model of the troposphere. Different parts of the drag can be separated from the numerical results; total pressure drag is determined from the surface pressure distribution, hydrostatic drag from the temperature distribution in the atmosphere, and form drag as a residual.

The dependence of the different parts of the drag on the main influencing parameters, such as geometric parameters, dynamical and thermal parameters, and the surface roughness, was given.

The results suggest the separation of form drag into two parts: a viscous form drag due to turbulent viscosity of the air, and a turbulent form drag due to additional production of turbulence in the vicinity (mainly in the Ice) of the obstacle. The distinction of different drag producing mechanisms will help in the task of parameterization. Parameterization using similarity theories is meaningful only for ensembles of obstacles.



LITERATURE REVIEW

The main result was that parameterization of pressure drag in terms of an effective roughness length using Rossby number similarity theory will be possible only for the two parts of the form drag. All other parts of the drag have no corresponding mechanisms in the homogenous boundary layer.

J. Blom, L. Wartena (1969) described the development of a turbulent boundary layer in a neutral atmosphere downwind of an abrupt change of surface roughness. Both a single change and two subsequent changes are treated.

For the treatment of a single abrupt change, a theory of Townsend forms the starting point. It is proved, according to this theory, that no surface layer adapted to the underlying surface roughness can exist behind the change. It is then shown how Townsend's theory can be modified in such a way that this discrepancy is removed.

The modified theory gives nearly the same velocity profile as does the original. However, it leads to greatly different values of the surface shear stress behind the change, a matter of importance in calculating turbulent transport.

It is shown that a correct evaluation of the height of the adapted layer is of importance for the determination of surface shear stress and roughness height from measured velocity profiles.



4. EXPERIMENTATION

4.1. GENERAL

It is common to come across many things in our everyday life i.e. Automobiles like cars, bikes, ships, airplanes, etc. We use different sizes and shapes of buildings, towers, hydraulic structures etc. These are basically, the objects which possess roughness and are affected by wind. From practical point of view, Experimental work based on these objects, is generally slight difficult to present in a laboratory. For this reason, in a laboratory a designed model of the parameters is required. In these experiments, we will be able to know that how the roughness of a surface can be the cause behind changing properties of flow characteristics. With partially satisfied conditions of rough surfaces or bodies, a number of correlations were developed by many investigators. The present study is intended to observe the effects of roughness, velocity distributions, boundary layer properties on flat plates and development of correlations which give a suitable value directly for the boundary layer parameters in turbulent zones.

For the present research work, to study the flow over the rough flat plate experimentally, the setup of wind tunnel available in the Hydraulic Machine Laboratory of the Civil Engineering Department, at the National Institute of Technology, Rourkela, India, were utilized. For better understanding of the variation of boundary layer parameters due to variation surface roughness, ambient velocities and distance from leading edge of the surface, is the basic objective behind these experiments.

4.2 WIND TUNNEL USED IN THE EXPERIMENT

The wind tunnel used in this project is a low speed wind tunnel in the Hydraulic Machines Laboratory located at National Institute of Technology, Rourkela, Odisha.

The highest speed of wind stream of the wind tunnel is up to 45m/s. The specifications of dimensions are tabulated as follows;

Table No. 4.2.1. Specification of Laboratory Wind Tunnel Components

COMPONENTS	LENGTH (m)	INLET (m)	OUTLET (m)
EFFUSER	1.3	2.1 × 2.1	2.1 × 2.1
TEST-SECTION	8	0.6 × 0.6	0.6 × 0.6
DIFFUSER	5	0.6	0.6



Fig. No. 4.2.1 Wind Tunnel used for the project



Fig. No. 4.2.2 Driving unit of the Wind Tunnel

4.3 EQUIPMENTS

Some of the principal equipments for carrying out of the experiment are discussed below.

- i. Digital Veloci Manometer
- ii. Telescopic pitot-tube
- iii. Rough flat Plates of different grades
- iv. Special trolley arrangement
- v. Tachometer

4.3.1. DIGITAL VELOCI-MANOMETER- This instrument is used for the velocity measurement purpose. Two rubber pipes, one for the static and other for the dynamic pressure head are attached to the meter. No battery is used in the instrument as this is operated directly by power; The Fig.No.4.3.1 shows the digital velocity meter used in this project.



Fig. No. 4.3.1 Digital velocitymeter

4.3.2. TELESCOPIC PITOT-TUBE- Telescope Pitot tube (Fig. No. 4.3.1) contains the velocity, humidity and temperature sensors; that measures velocity within test section of wind-tunnel at different height from surface. Use of the probe makes possible that the orientation dimple is facing upstream and sensor opening is fully exposed.



Fig. No. 4.3.2 Telescopic Pitot-Tube

4.3.3. ROUGH FLAT PLATES- Before the experimentation, the rough flat plates were prepared. Roughness on the flat plates were introduced using emery papers. The grades of roughness indicate the size of grains of the emery paper.

For increasing diameter of grains, there is increase in roughness of emery paper. In such way, the 40 grade roughness plate has rougher surface than that of 50, 60 & 120 grades. (Fig. No. 4.3.3 (a) and (b)). These are pasted on the wooden flat plates with the help of gum.



Fig. No. 4.3.3(a) Rough surfaces of grade 40(375 μ m) and 50(345 μ m)



Fig. No. 4.3.3(b) Rough surfaces of grade 60(290 μ m) and 120(125 μ m)

Table No. 4.3.1

FLAT PLATE GEOMETRY	DIMENSION
Length	100cm
Breadth	50cm
Thickness	12mm
Material	wood

Table No. 4.3.2

GRADES OF ROUGH SURFACE	ROUGHNESS HEIGHT
40	375 μm
50	345 μm
60	290 μm
120	125 μm

4.3.4. SPECIAL TROLLEY ARRANGEMENT- Here in wind tunnel, Trolley is basically used for the movement of Pitot tube. Taking velocity readings from a section to other becomes easier due to the Trolley arrangement. This special type of trolley (Fig. No. 4.3.4) was arranged for this work to take the readings parallel to the surface.



Fig. No. 4.3.4 Special Trolley Arrangement

4.3.5. TACHOMETER- The device is being used for the assistance in measuring the rotations per minute of the shaft in the driving unit of the wind tunnel. These records of making changes in the speed of wind tunnel are required because for each grades of plate, the same free stream velocities are to be set. Therefore the work goes on easier if the rpm values are recorded. The tachometer used in the laboratory is shown in Fig.No.4.2.5.



Fig. No. 4.3.5 Digital Laser Tachometer

4.4. SET-UP

- At first the experimental set-up consists of the trolley arrangement attached with telescopic pitot-tube with it.
- The pitot-tube is to be inserted into the test section from the little rectangular space located above the section.
- Then the rough flat plate of grade 40 ($375\mu\text{m}$) is introduced inside the test section and kept on an iron stand of 30cm height.
- The tip of the sensor of pitot tube is to be placed carefully facing the upstream, -along the center line sections created on the rough flat plate.
- At last but not the least, the spaces above the test section around the pitot-tube are to be blocked by small & thin pieces of wooden plates.
- Fig.No.4.4.1 shows the test section of the wind tunnel where the flat plate was placed on the Iron bench for our experiment.



Fig no.4.4 Test Section of the experiment



5. METHODOLOGY

- The speed of the free stream was set to a particular desired value of velocity by settling the motor into a constant rpm by observing the tachometer readings.
- Then the free stream velocity (V_1) inside empty test-section at room temperature (25^0 to 27^0C) was measured by the Veloci-manometer & noted down.
- For the current free stream velocity, the velocities above each center-lined section are to be tabulated carefully.
- The centerline of flat plate is marked & 17 sections at 5cm intervals from the leading edge are also marked neatly.
- The plate was finally adjusted and placed in such a way that the tip of pitot-tube can be moved smoothly throughout along the marked centerline by the trolley.
- The velocity measurements were taken at each section from bed level to the height up to which the free stream velocity is achieved and becomes constant. The pitot-tube was raised at interval of 0.2mm & later the distance is increased to 0.5mm.
- The above procedure was carried out for all the 17 sections (however only turbulent zone sections were required) by moving the trolley carefully and all the velocity readings along with corresponding heights were recorded.
- Now the speed of the free stream is to be set into another value of rpm by means of tachometer to get the next free stream velocity (V_2).
- Then all the previous procedures were repeated. Provided that this test is done or zero pressure gradient.
- This experiment was done for three different constant free-stream velocities; viz. 10.9m/s, 12.5m/s and 13.6m/s. then the tabulated data were supposed to be used for plot - Of graphs and further observations.

6. EXPERIMENTAL RESULTS

6.1. OVERVIEW

The results of experiments about the velocity profiles, the variations of boundary layer parameters with respect to the main-stream velocities and roughness profiles are presented in this chapter. Analysis is also done for calculation of required parameters and plots are shown. The overall summary of experiment runs for a brief explanation of the characteristics of boundary layer responses in turbulent zone.

The results of these tests are represented in this chapter, in terms of velocity profiles in numerous ways to serve different purposes.

- ✓ From the experimental data the graphs of velocity profiles are plotted first.
- ✓ Then graphs for v vs y at different free-stream velocities for a particular section in turbulence zone were shown.
- ✓ Velocity variations for different roughness were analyzed at every free-stream velocity.
- ✓ Here we observed the regularity and variations in the patterns for increasing velocities with the rise in vertical height at different sections in the zone of turbulence.

6.2. VELOCITY PROFILES

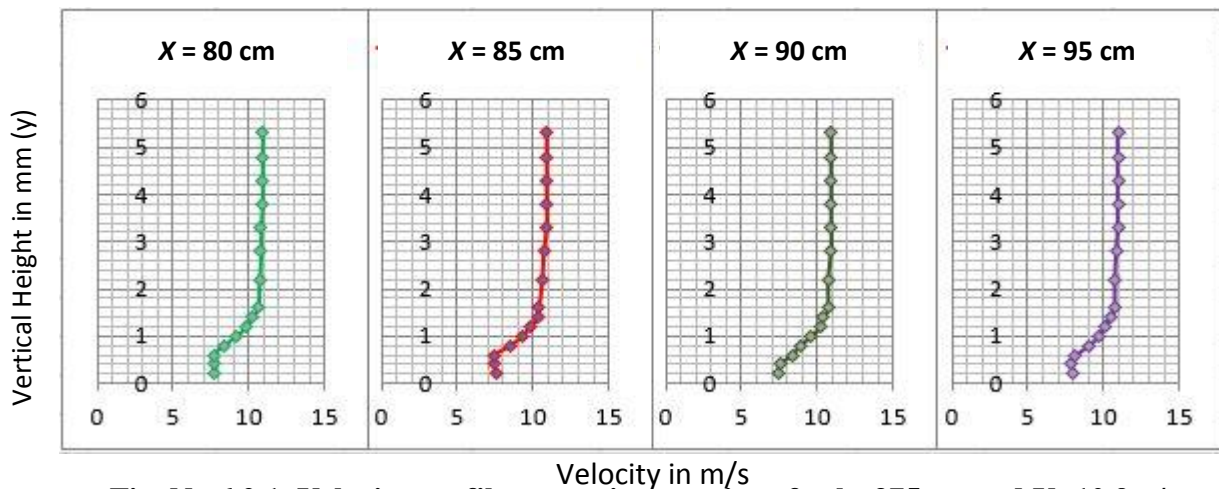


Fig. No.6.2.1. Velocity profiles at various sections for $k=375\mu\text{m}$ and $V=10.9\text{m/s}$

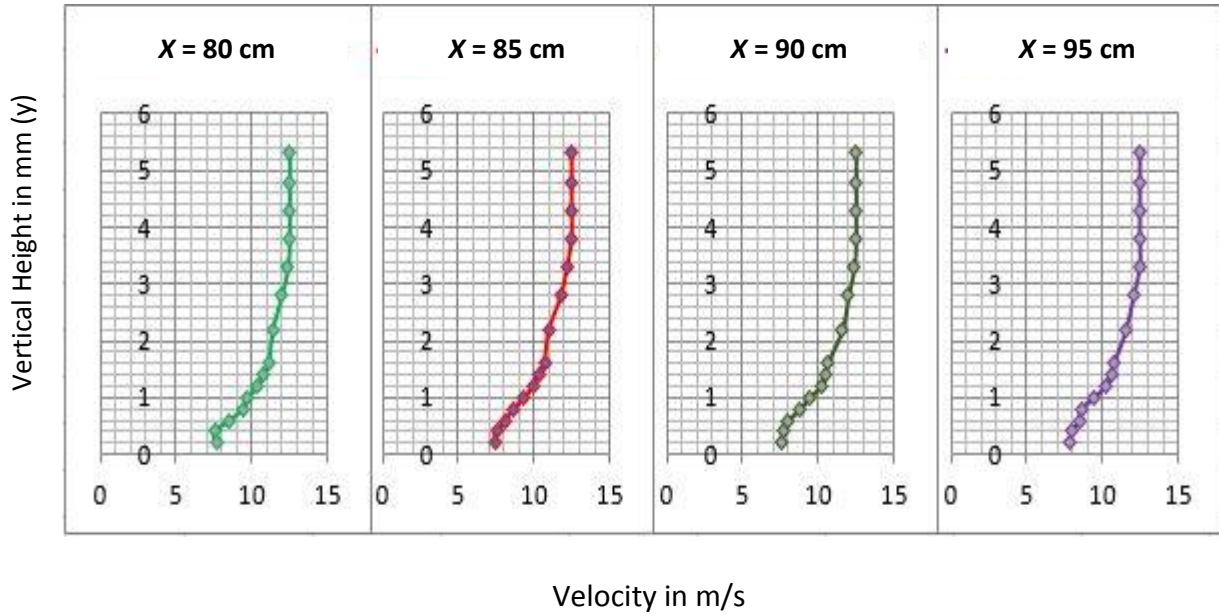


Fig. No.6.2.2. Velocity profiles at various sections for $k=375\mu\text{m}$ and $V=12.5\text{m/s}$

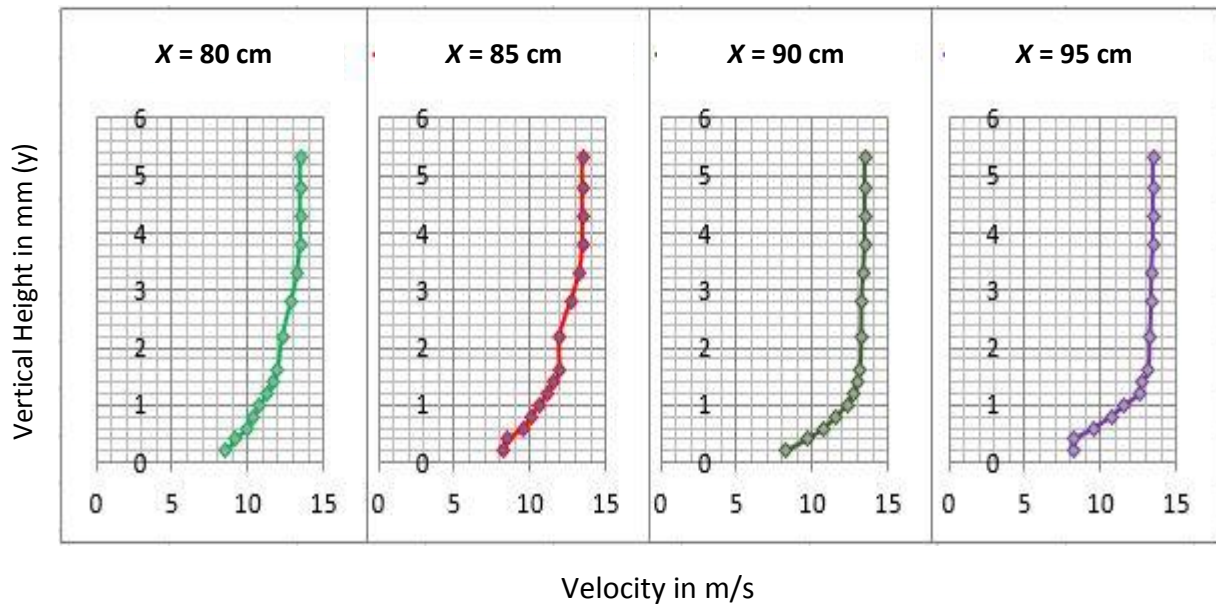


Fig. No.6.2.3. Velocity profiles at various sections for $k=375\mu\text{m}$ and $V=13.6\text{m/s}$

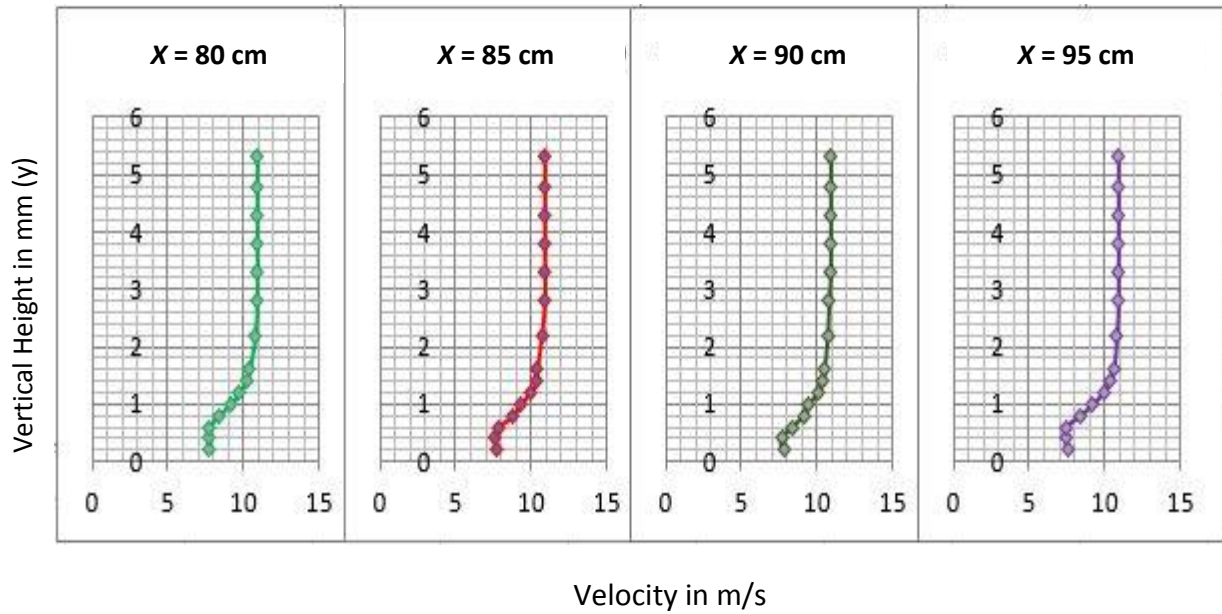


Fig. No.6.2.4. Velocity profiles at various sections for $k=345\mu\text{m}$ and $V=10.9\text{m/s}$

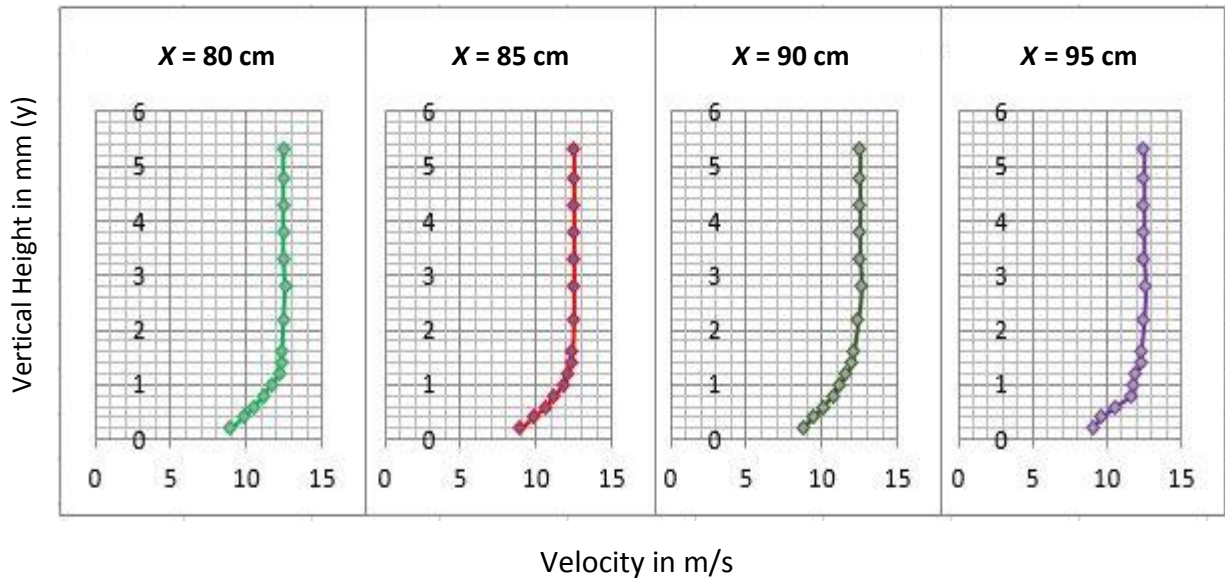


Fig. No.6.2.5. Velocity profiles at various sections for $k=345\mu\text{m}$ and $V=12.5\text{m/s}$

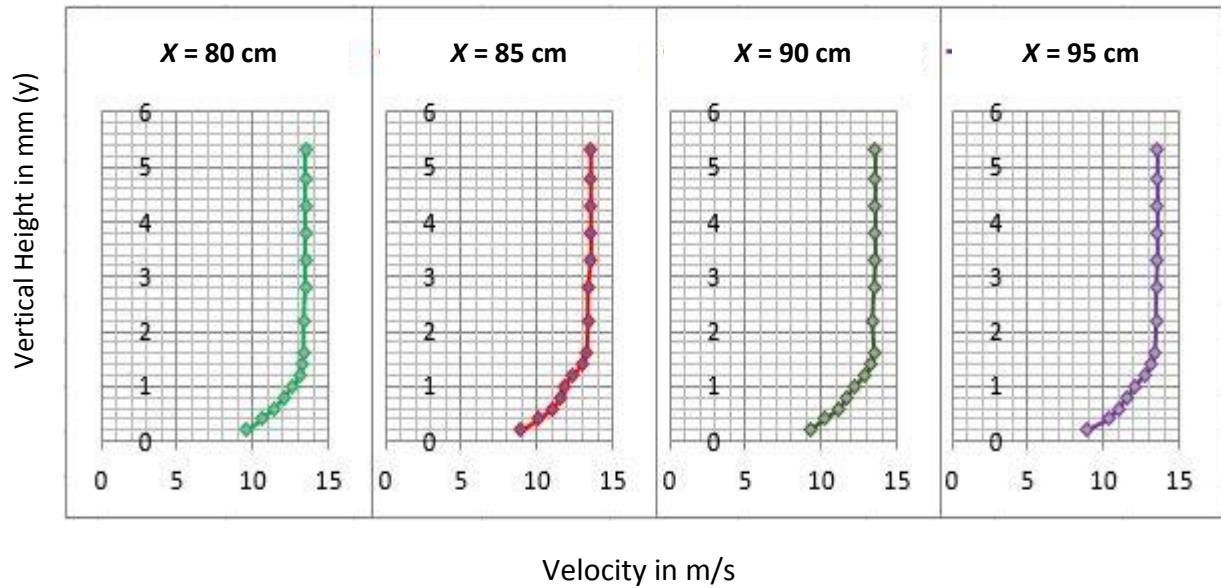


Fig. No.6.2.6. Velocity profiles at various sections for $k=345\mu\text{m}$ and $V=13.6\text{m/s}$

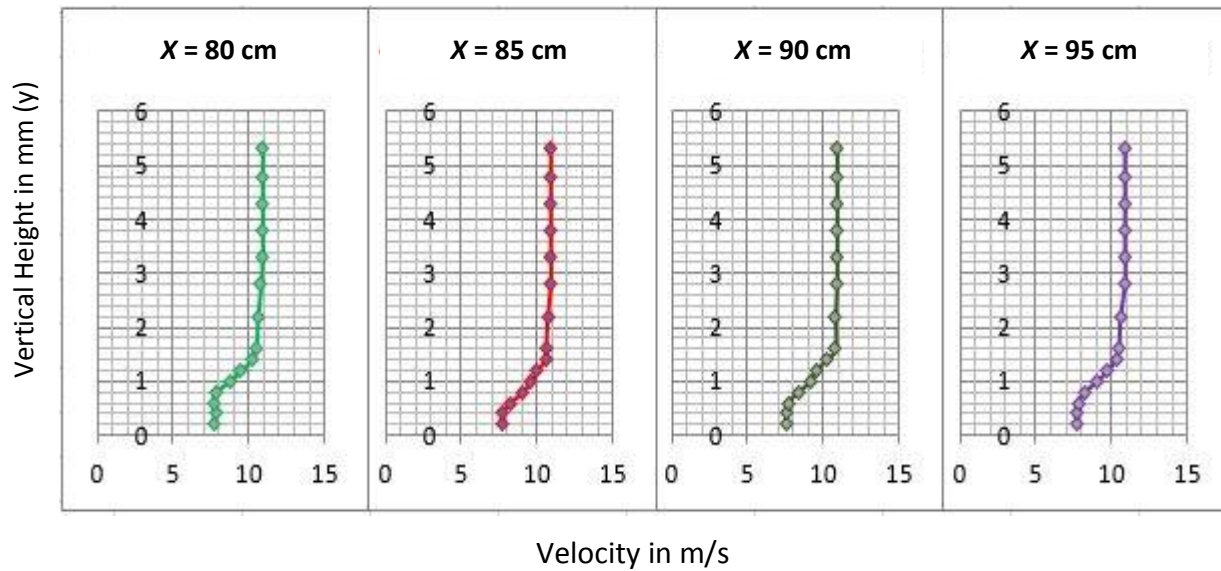


Fig. No.6.2.7. Velocity profiles at various sections for $k=290\mu\text{m}$ and $V=10.9\text{m/s}$

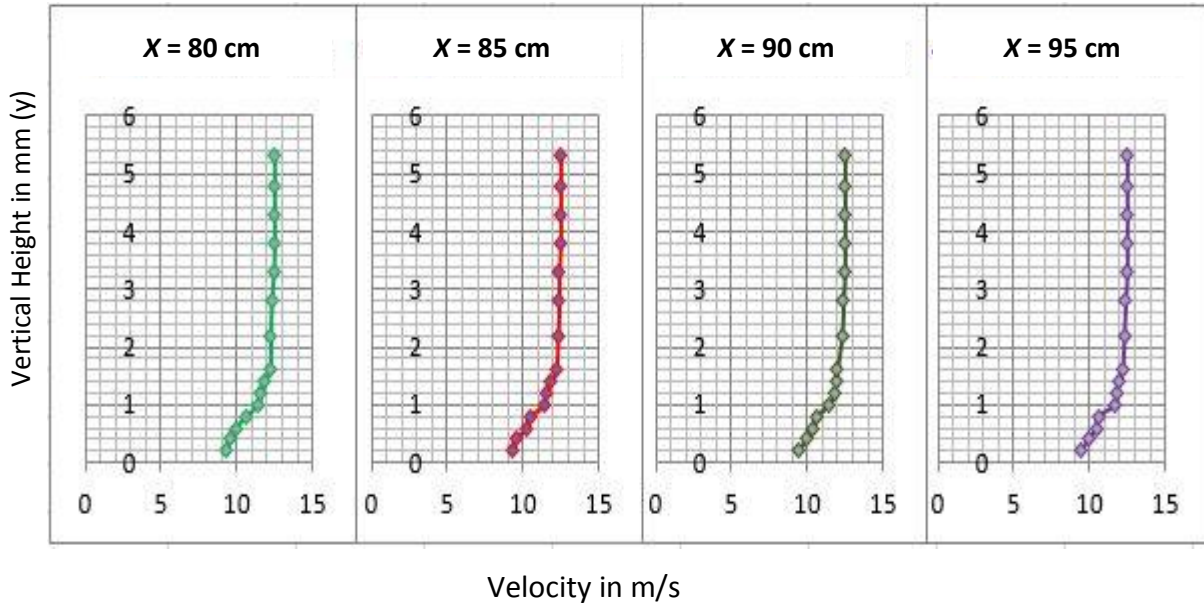


Fig. No.6.2.8. Velocity profiles at various sections for $k=290\mu\text{m}$ and $V=12.5\text{m/s}$

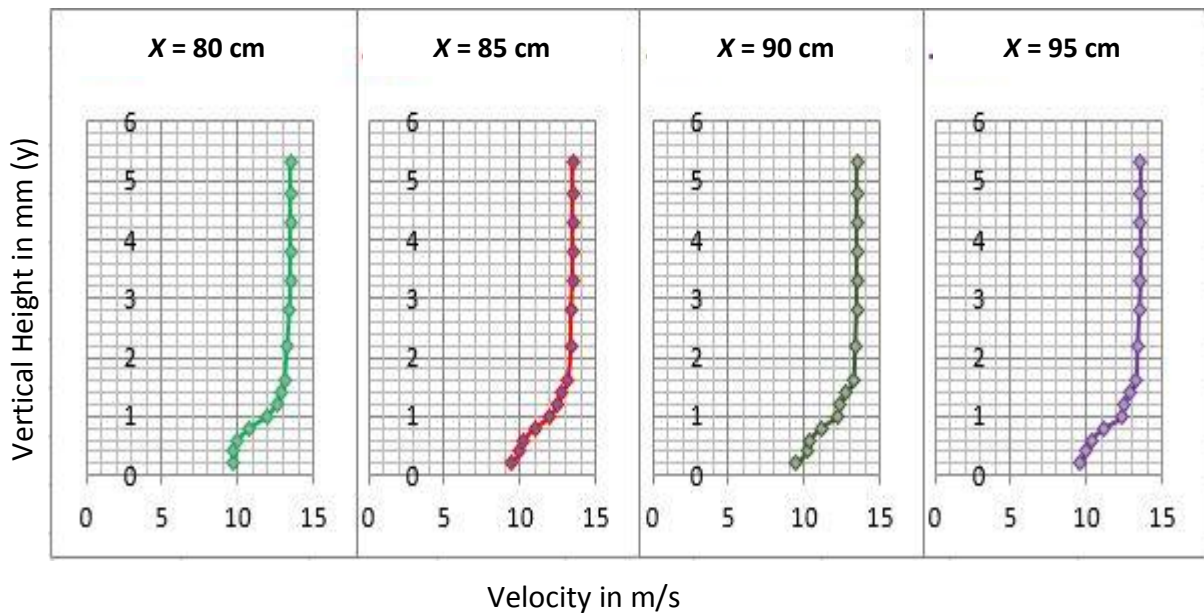


Fig. No.6.2.9 Velocity profiles at various sections for $k=290\mu\text{m}$ and $V=13.6\text{m/s}$

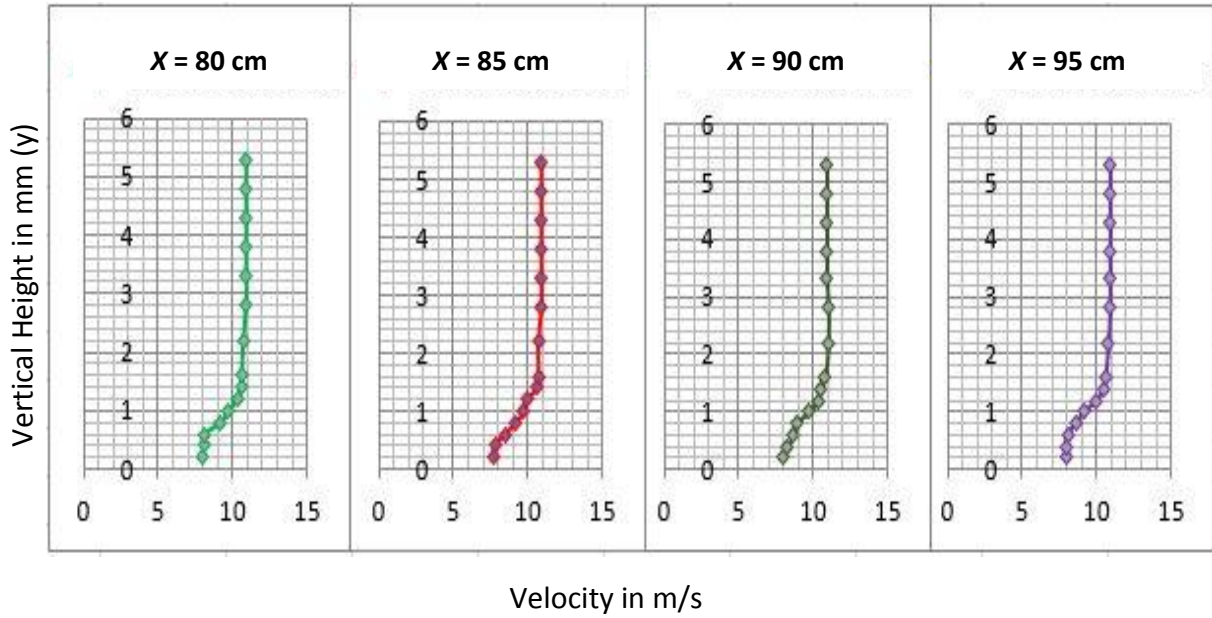


Fig. No.6.2.10. Velocity profiles at various sections for $k=125\mu\text{m}$ and $V=10.9\text{m/s}$

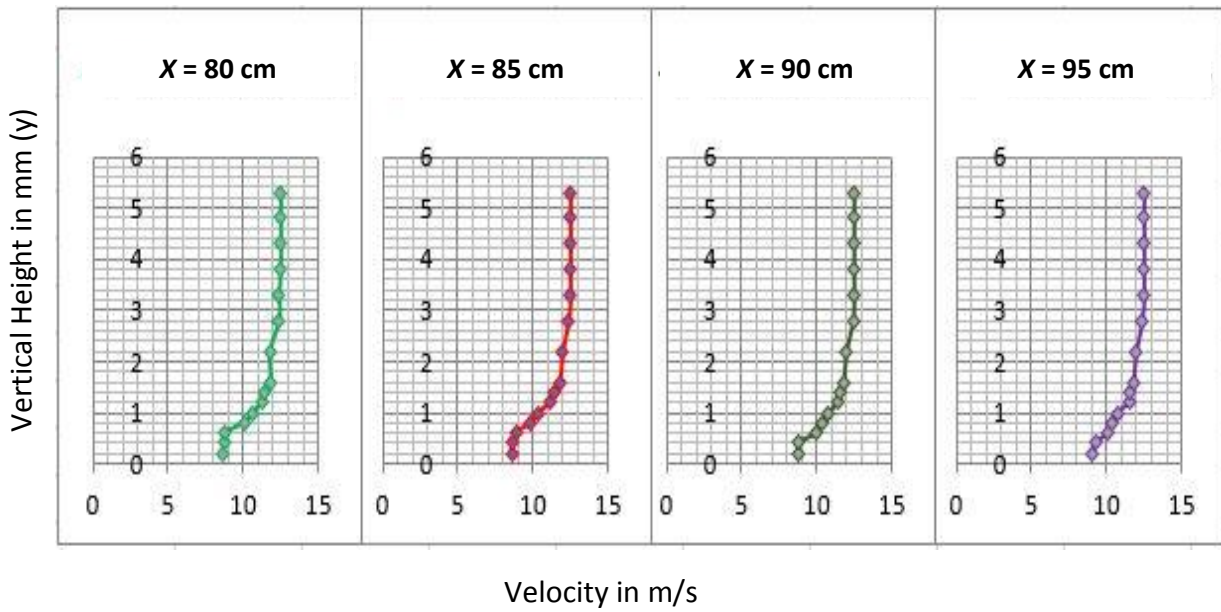


Fig. No.6.2.11. Velocity profiles at various sections for $k=125\mu\text{m}$ and $V=12.5\text{m/s}$

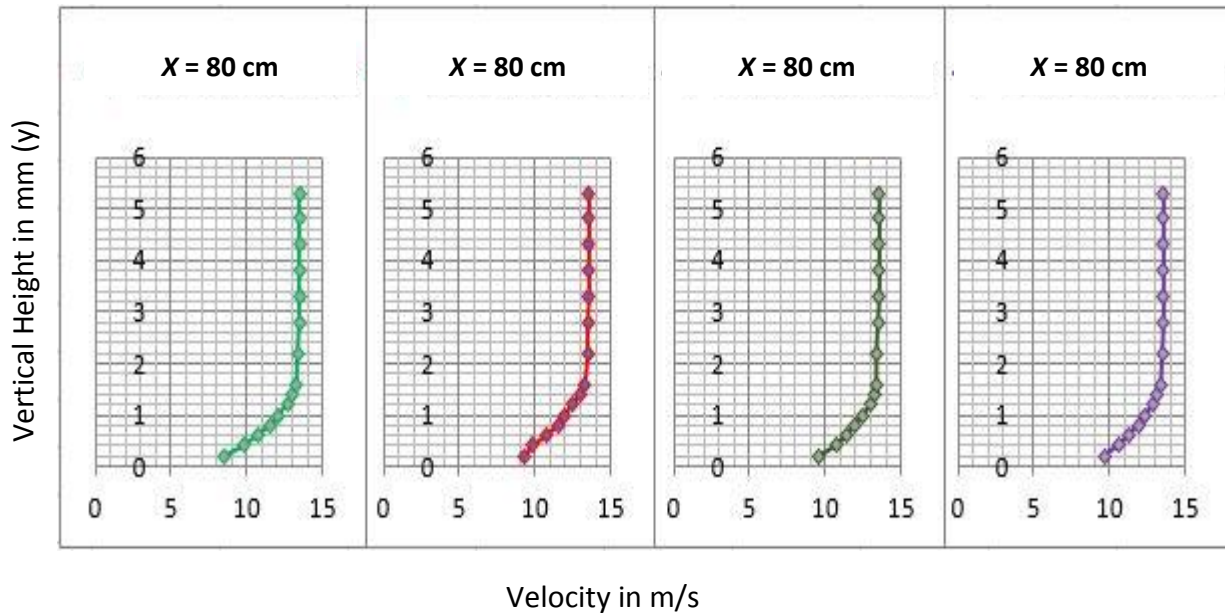


Fig. No.6.2.12. Velocity profiles at various sections for $k=125\mu\text{m}$ and $V=13.6\text{m/s}$

These are the velocity profiles shown above for the different main stream velocities at different sections taken along the center line of the rough flat plate surface, in the zone of turbulent boundary layer.

6.3. VELOCITY VARIATIONS AT A PARTICULAR SECTION AND ROUGHNESS FOR CHANGING MAIN STREAM VELOCITIES

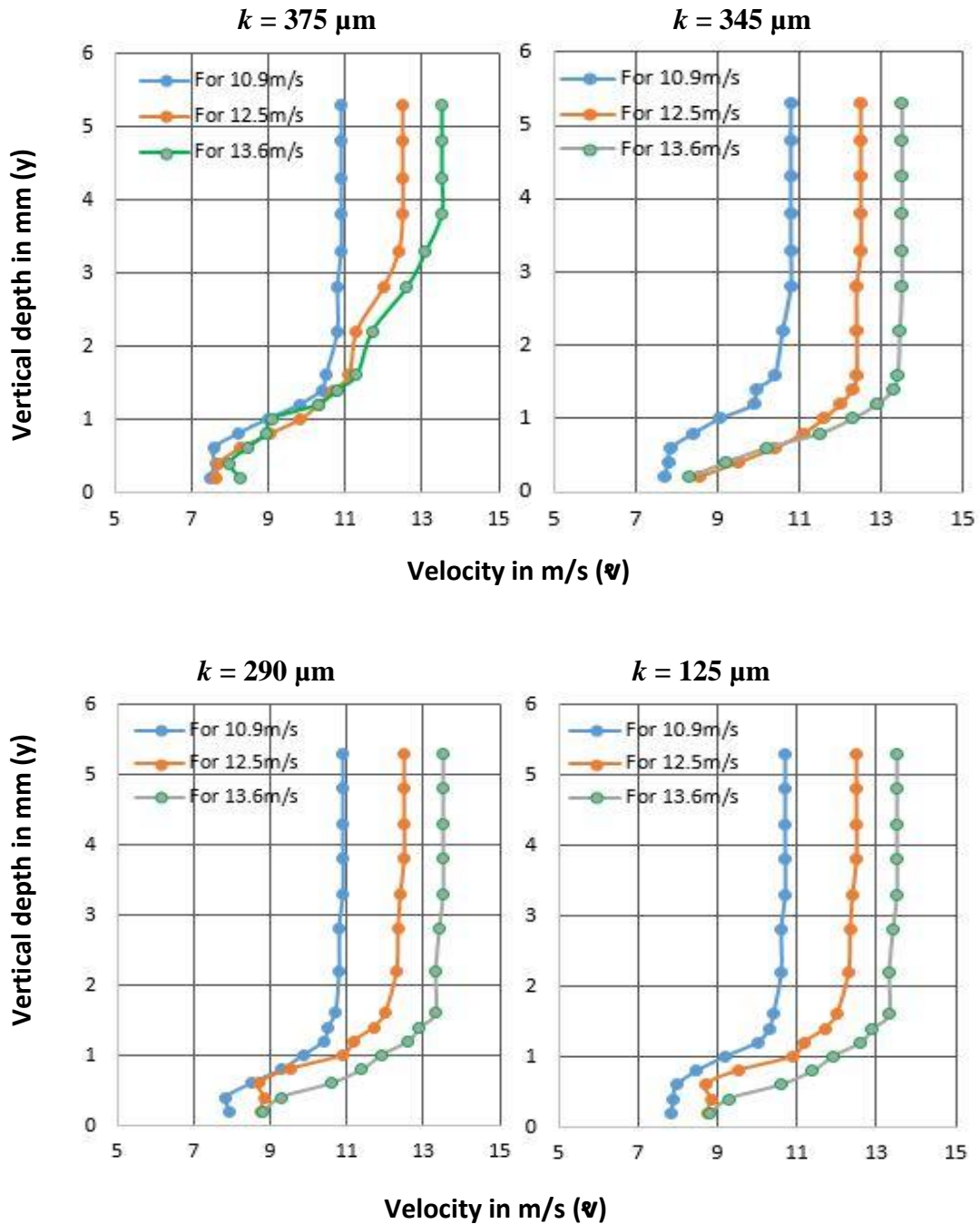


Fig No. 6.3.1. Velocity Profiles At section $x=70\text{cm}$ for varying Main-stream velocities

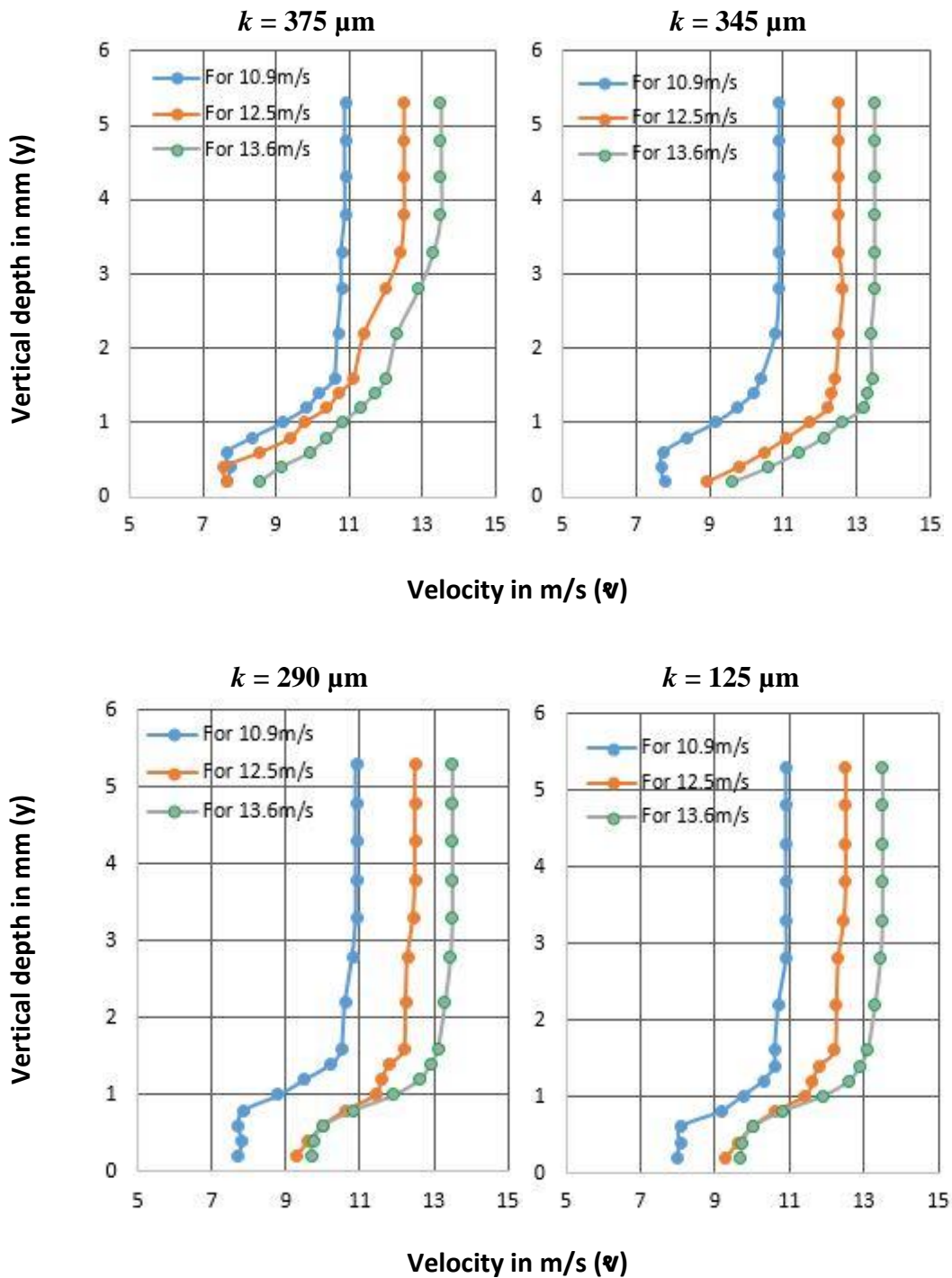


Fig No. 6.3.2. Velocity Profiles At section $x=80\text{cm}$ for varying Main-stream velocities

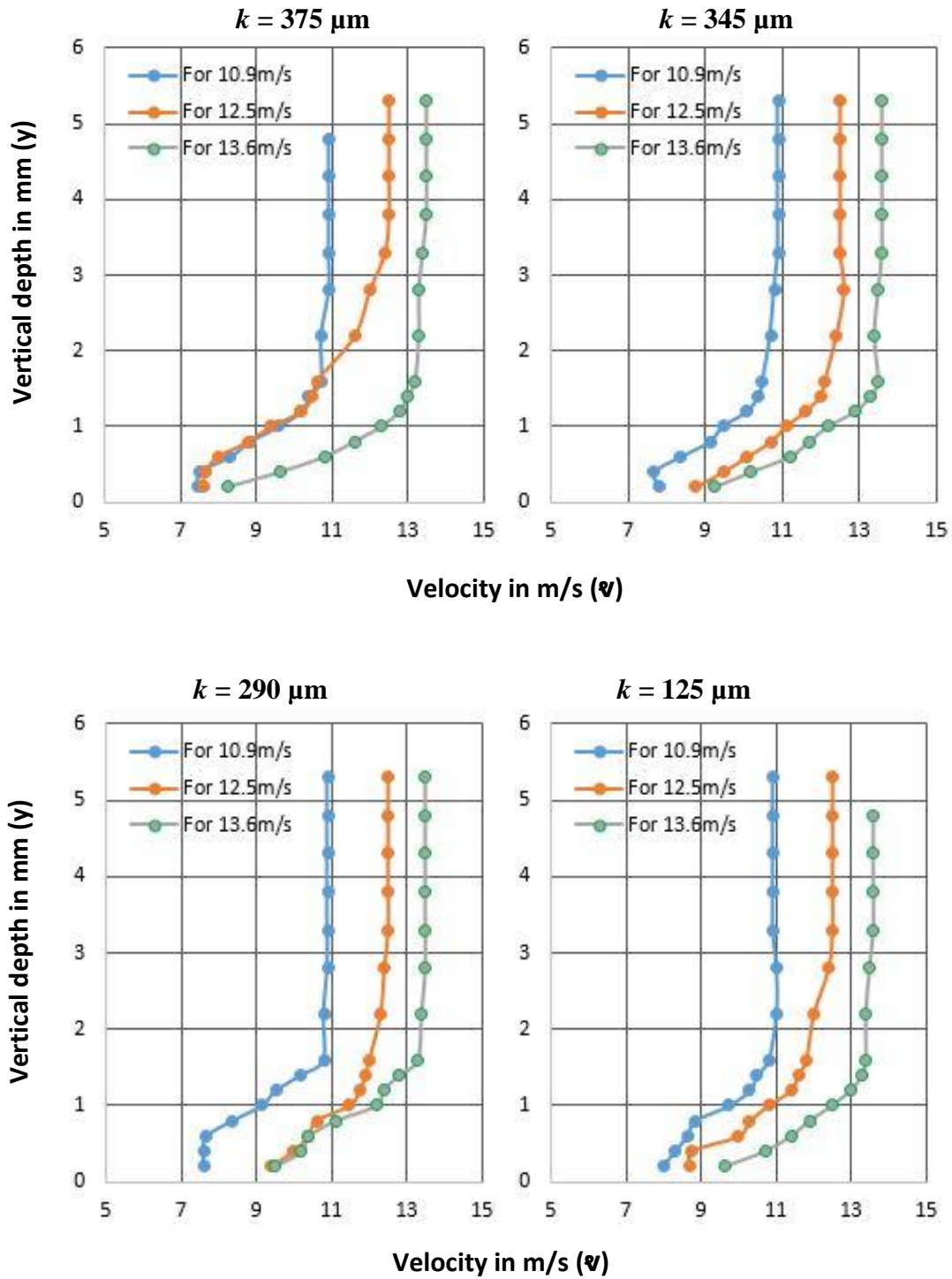


Fig No. 6.3.3. Velocity Profiles At section x=90cm for varying Main-stream velocities

6.4. VELOCITY VARIATIONS AT A PARTICULAR SECTION AND FREE-STREAM VELOCITY FOR CHANGING ROUGHNESS

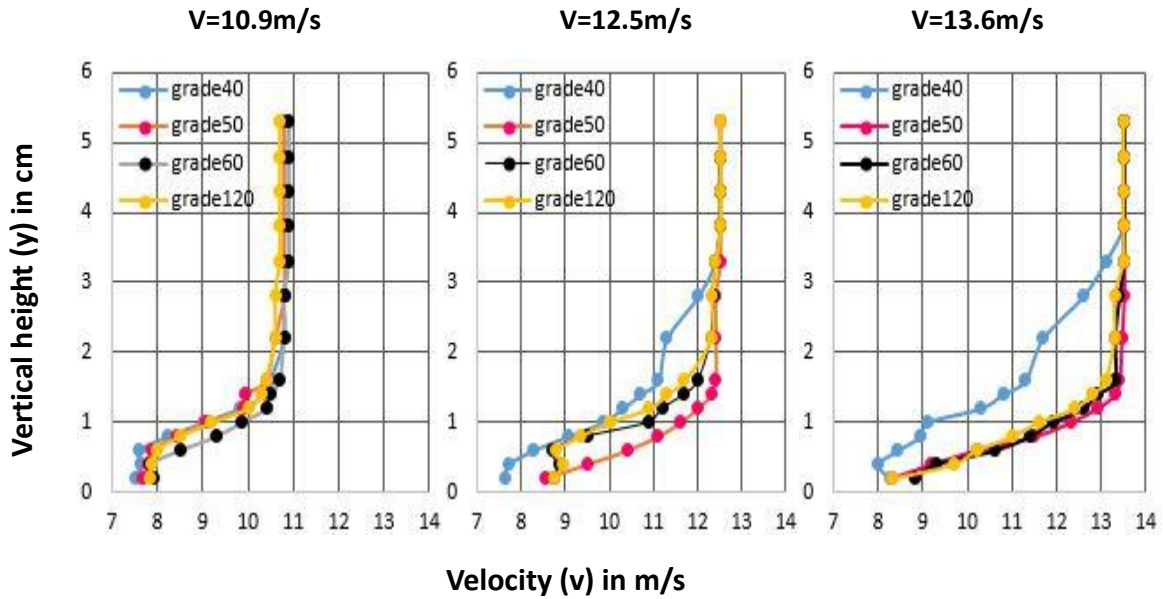


Fig. No.6.4.1. Velocity Variations At $x=70\text{cm}$ for varying free-stream velocities

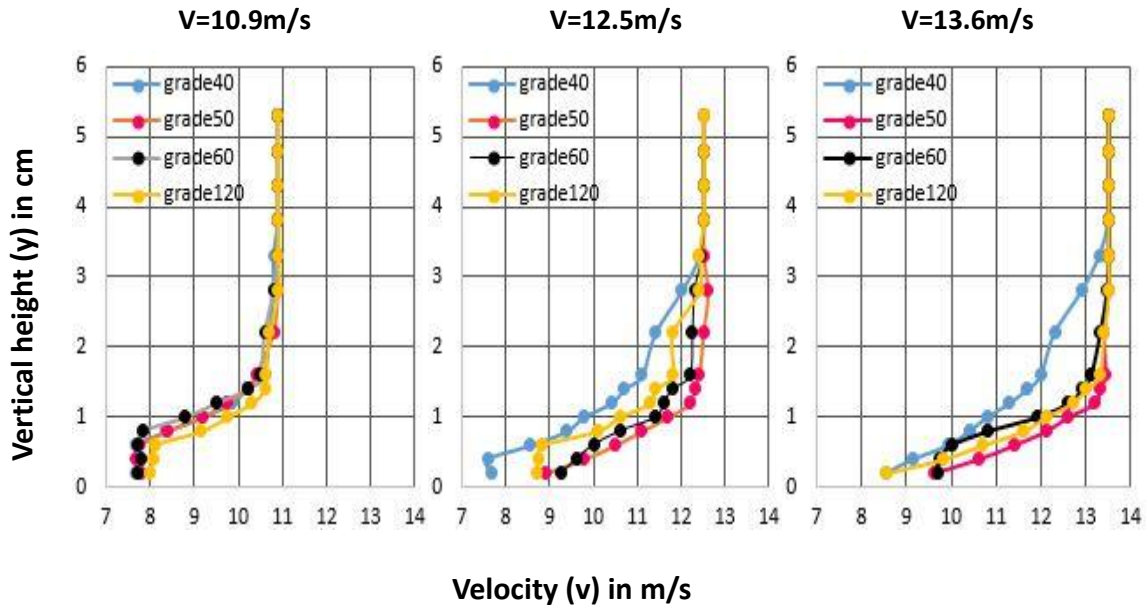


Fig. No.6.4.2. Velocity Variations At $x=80\text{cm}$ for varying free-stream velocities

6.5. BOUNDARY LAYER GROWTH

The B/L growth was shown only for the zone of turbulence as per the requirement of this project. The sections lying under the turbulent region of the plate were known from the relation of Reynold’s number (R_e), which is given by,

$$R_e = \frac{V \times x}{\nu}$$

Where, R_e = Reynold’s No, for turbulent flow it is 5×10^5

V = Main-stream Velocity in m/s

x = Distance from the leading edge of the plate in cm

ν = Kinematic viscosity of fluid (for air $16 \times 10^{-6} \text{m}^2/\text{s}$ at room temperature 27°C)

6.5.1. BOUNDARY LAYER VARIATIONS AT CONSTANT FREE STREAM VELOCITY FOR VARYING ROUGHNESSES

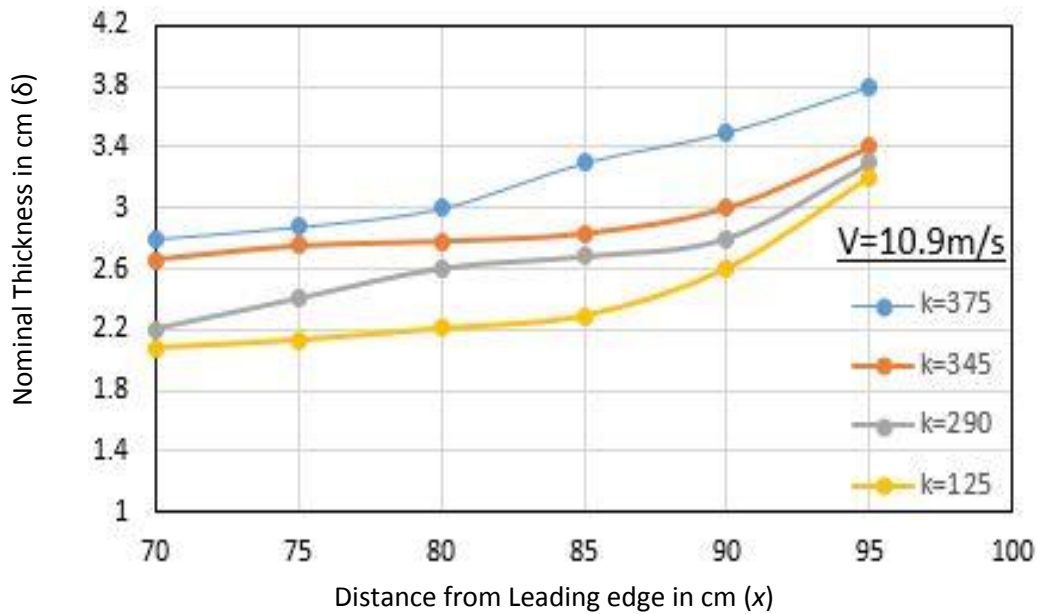


Fig. No.6.5.1 (a) Boundary layer growth in Turbulent B/L zone for $V=10.9 \text{m/s}$

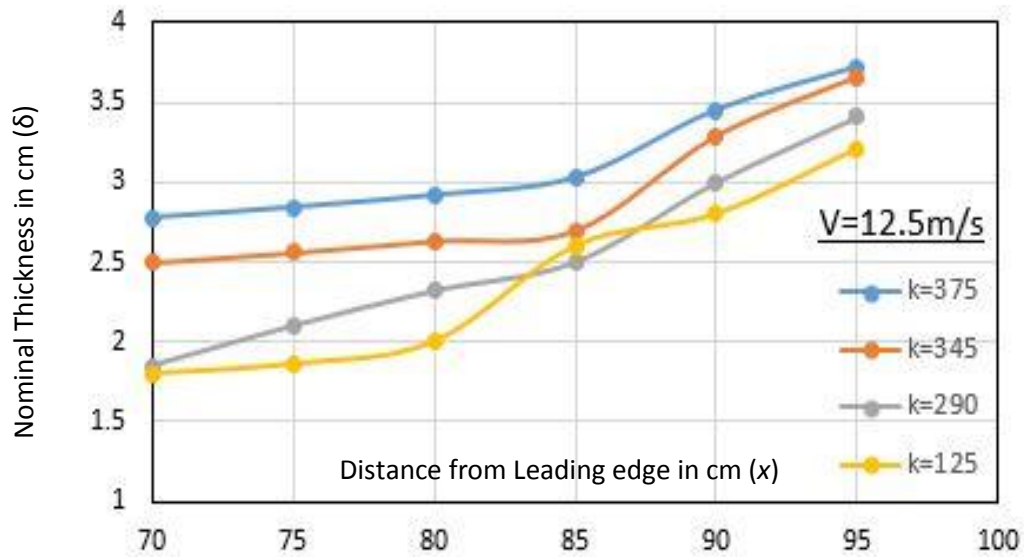


Fig. No.6.5.1 (b) Boundary layer growth in Turbulent B/L zone for V=12.5m/s

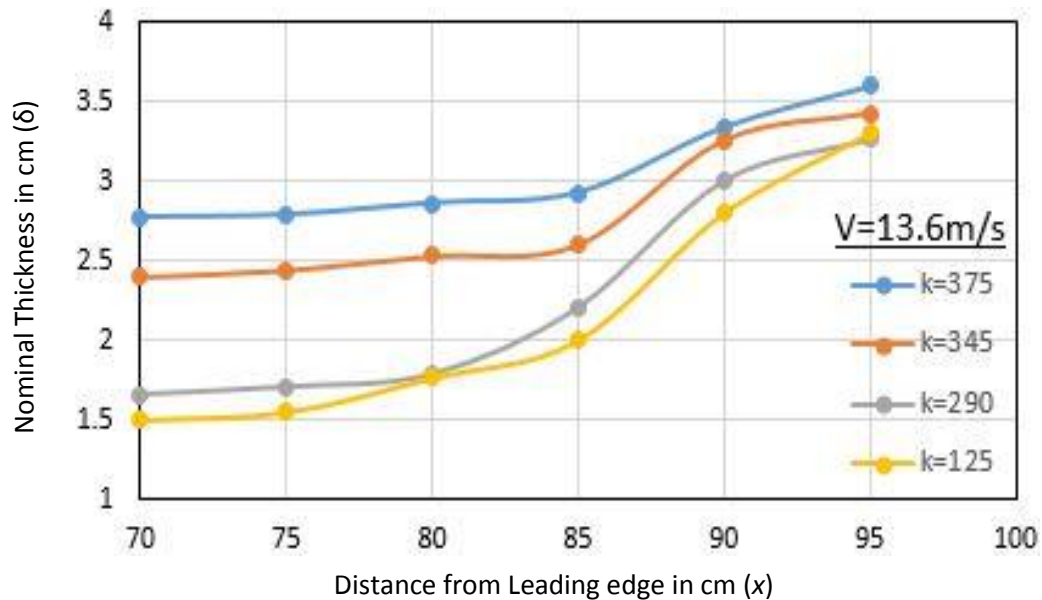


Fig. No.6.5.1 (c) Boundary layer growth in Turbulent B/L zone for V=13.6m/s

6.5.2. BOUNDARY LAYER VARIATIONS AT CONSTANT ROUGHNESS FOR VARYING FREESTREAM VELOCITIES

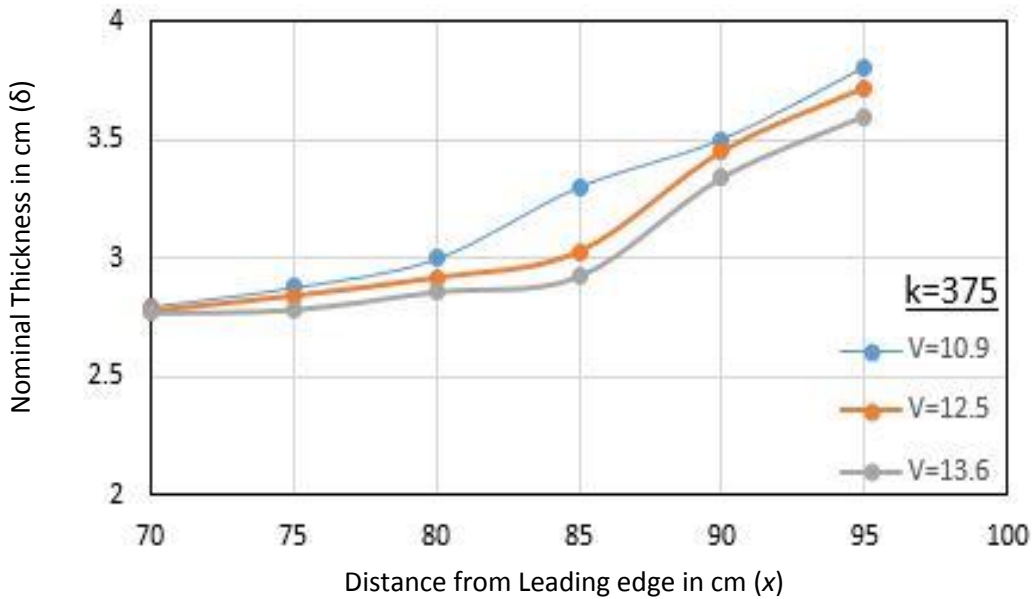


Fig. No.6.5.2 (a) Boundary layer growth in Turbulent B/L zone for k=375 μm

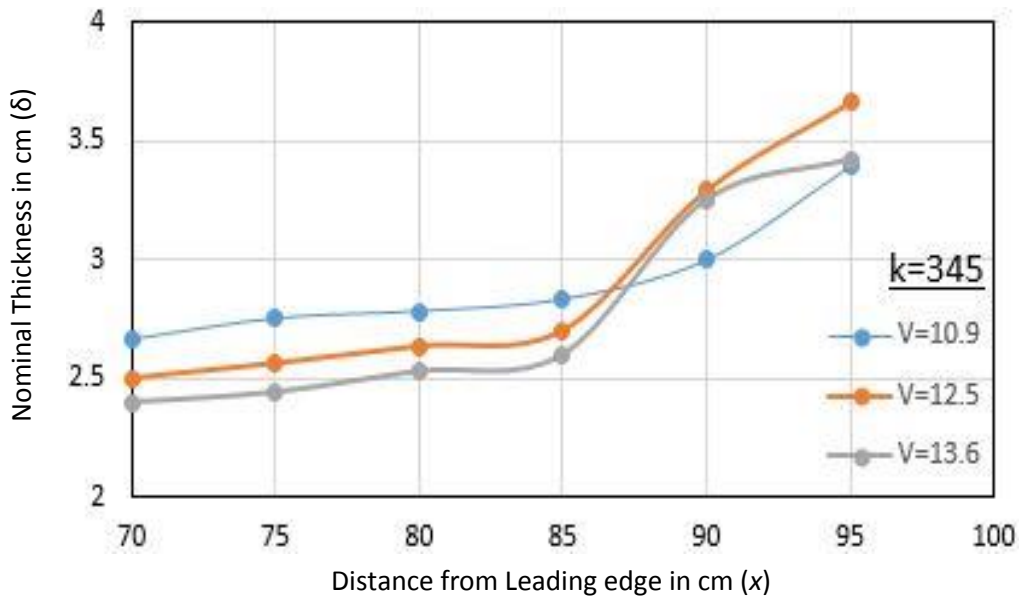


Fig. No.6.5.2 (b) Boundary layer growth in Turbulent B/L zone for k=345 μm

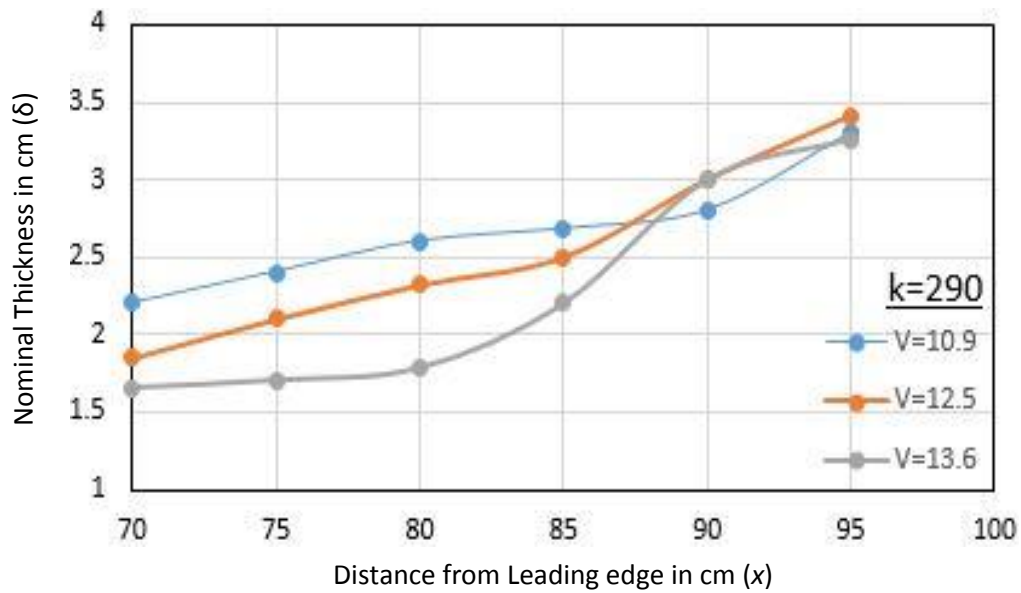


Fig. No.6.5.2 (c) Boundary layer growth in Turbulent B/L zone for $k=290\mu\text{m}$

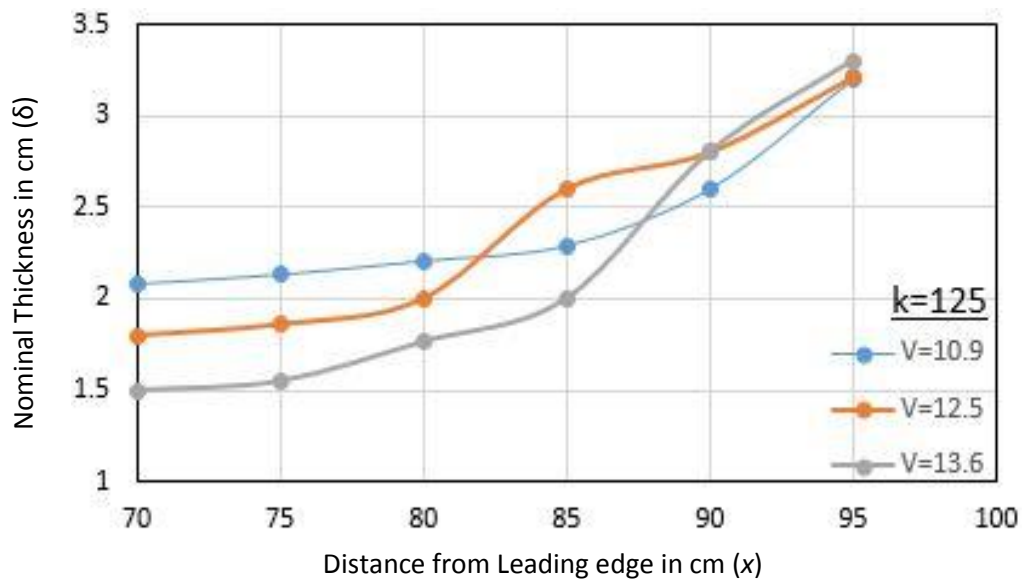


Fig. No.6.5.2 (d) Boundary layer growth in Turbulent B/L zone for $k=125\mu\text{m}$



6.6. CALCULATIONS OF PARAMETERS

From experiments and the graphical analysis the equations obtained were used to determine the parameters of the boundary layer in the turbulent boundary layer zones. Following approaches have given their contribution to obtain the desired parameters and the respective correlations.

6.6.1. DETERMINATION OF BOUNDARY LAYER PARAMETERS

All the equations obtained from the $\frac{y}{\delta}$ vs. $\frac{v}{V}$ Plots are in the following quadratic form of $(-ax^2+bx+c)$. So for easy and convenient calculations the integrations for different parameters are integrated for the above form and formulised.

For displacement thickness (δ^*);

$$\begin{aligned}\delta^* &= \int_0^{\delta} \left(1 - \frac{v}{V}\right) dy \\ \Rightarrow \delta^* &= \int_0^{\delta} (-ax^2 + bx + c) dy \\ \Rightarrow \delta^* &= \left[1 + \frac{a}{3} - \frac{b}{2} - c\right] \times \delta\end{aligned}$$

Where δ = Boundary layer thickness in cm

a, b, c are the co-efficient of x^2 , x and constant term in the Quadratic equations respectively.

For momentum thickness (θ);

similarly,

$$\begin{aligned}\theta &= \int_0^{\delta} \frac{v}{V} \left(1 - \frac{v}{V}\right) dy \\ \Rightarrow \theta &= \left[-\frac{a}{3} + \frac{b}{2} + c - \frac{a^2}{5} - \frac{b^2}{3} - c^2 + \frac{ab}{2} - bc + \frac{2ca}{3}\right] \times \delta\end{aligned}$$

For energy thickness (δ_E);

$$\delta_E = \int_0^\delta \frac{v}{V} \left(1 - \frac{v^2}{V^2}\right) dy$$

$$\Rightarrow \delta_E = \left[\frac{-a}{3} + \frac{b}{2} + c + \frac{a^3}{7} - \frac{b^3}{4} - c^3 - \frac{a^2b}{2} + \frac{3ab^2}{5} - b^2c - \frac{3bc^2}{2} + c^2a - \frac{3ca^2}{5} + \frac{3abc}{2} \right] \times \delta$$

Then further computations and results were proceeded, a sample calculation along with other values are shown below;

1. For $\frac{y}{\delta}$ vs. $\frac{v}{V}$ at $V=10.9\text{m/s}$, $x = 85\text{cm}$ and;

a) $k=375\mu\text{m}$

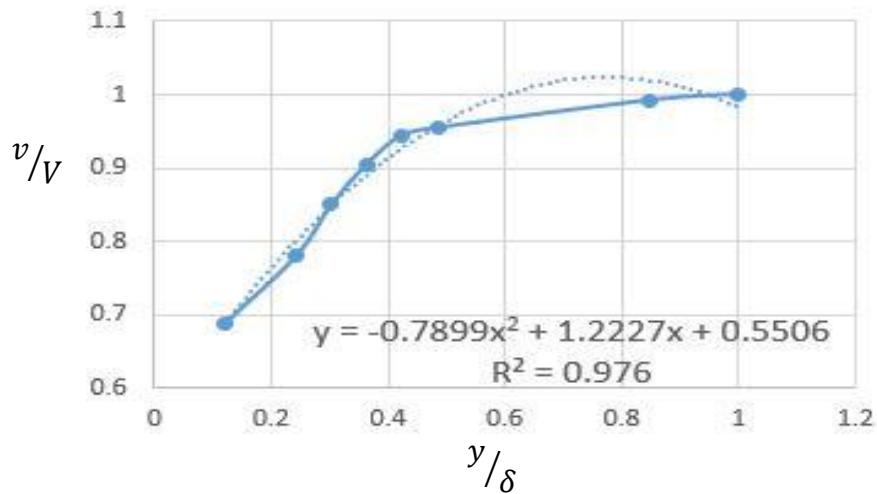


Fig. No. 6.6.1 (a)

$$\frac{v}{V} = -0.7899 \left(\frac{y}{\delta}\right)^2 + 1.2227 \left(\frac{y}{\delta}\right) + 0.5506$$

Here, $a = 0.7899$, $b = 1.2227$, $c = 0.5506$, $\delta = 3.3\text{cm}$



RESULTS AND DISCUSSION

Now,

$$\delta^* = \left[1 + \frac{0.7899}{3} - \frac{1.2227}{2} - 0.5506 \right] \times 3.3 = 0.34 \text{ cm}$$

$$\theta = \left[-\frac{0.7899}{3} + \frac{1.2227}{2} + 0.5506 - \frac{0.7899^2}{5} - \frac{1.2227^2}{3} - 0.5506^2 + \frac{0.7899 \times 1.2227}{2} - (1.2227 \times 0.5506) + \frac{(2 \times 0.5506 \times 0.7899)}{3} \right] \times 3.3$$

$$= 0.2376 \text{ cm}$$

$$\delta_E = \left[\frac{-0.7899}{3} + \frac{1.2227}{2} + 0.5506 + \frac{0.7899^3}{7} - \frac{1.2227^3}{4} - 0.5506^3 - \frac{(0.7899^2 \times 1.2227)}{2} + \frac{(3 \times 0.7899 \times 1.2227^2)}{5} - (1.2227^2 \times 0.5506) - \frac{(3 \times 1.2227 \times 0.5506^2)}{2} + (0.5506^2 \times 0.7899) - \frac{(3 \times 0.5506 \times 0.7899^2)}{5} + \frac{(3 \times 0.7899 \times 1.2227 \times 0.5506)}{2} \right] \times 3.3$$

$$= 0.409 \text{ cm}$$

b) $k=345\mu\text{m}$

Similarly for $k=345\mu\text{m}$,

$$a = 0.4324, b = 0.7894, c = 0.6405, \delta = 2.8 \text{ cm}$$

$$\delta^* = 0.315 \text{ cm}$$

$$\theta = 0.2376 \text{ cm}$$

$$\delta_E = 0.509 \text{ cm}$$

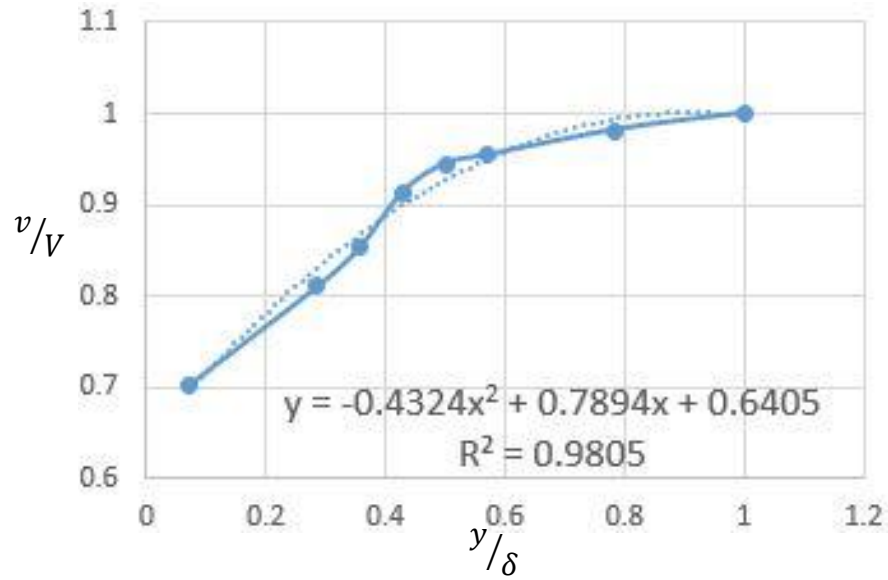


Fig. No. 6.6.1 (b)

c) $k=290\mu\text{m}$

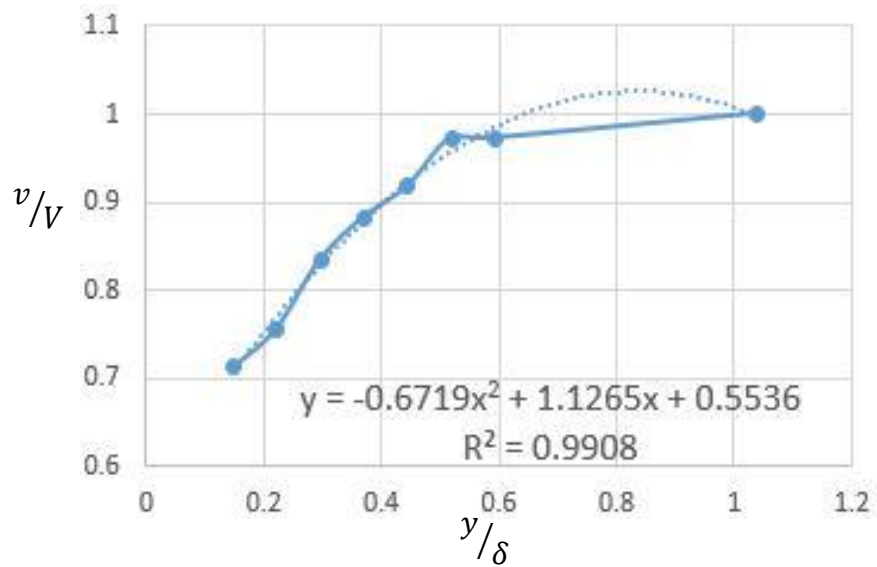


Fig. No. 6.6.1 (c)



RESULTS AND DISCUSSION

Similarly for $k=290\mu\text{m}$,

$$a = 0.6719, b = 1.1265, c = 0.5536, \delta = 2.6\text{cm}$$

$$\delta^* = 0.307\text{cm}$$

$$\theta = 0.2198\text{cm}$$

$$\delta_E = 0.4556\text{cm}$$

d) $k=125\mu\text{m}$

Similarly for $k=125\mu\text{m}$,

$$a = 0.5925, b = 1.0282, c = 0.5471, \delta = 2.2\text{cm}$$

$$\delta^* = 0.266\text{cm}$$

$$\theta = 0.1974\text{cm}$$

$$\delta_E = 0.3395\text{cm}$$

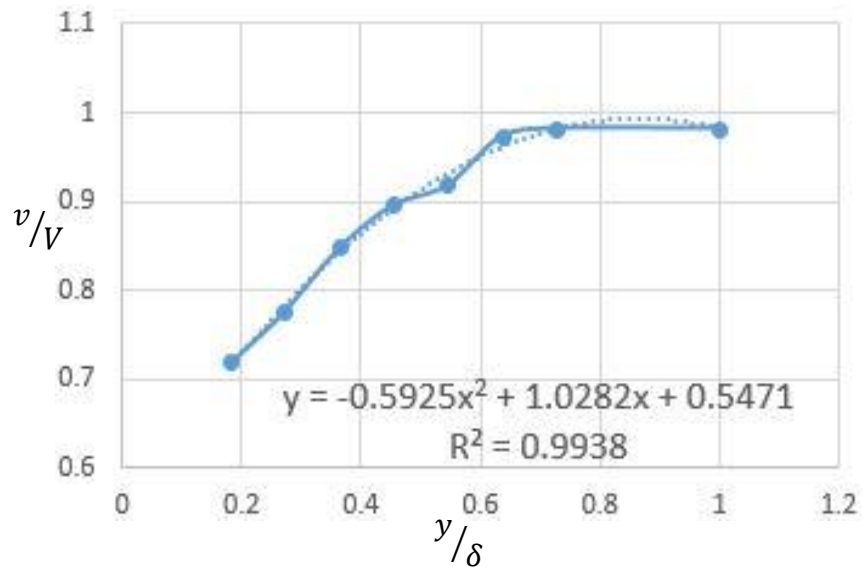


Fig. No. 6.6.1 (d)

2. For $\frac{y}{\delta}$ vs. $\frac{v}{V}$ at $k=375\mu\text{m}$, $x = 85\text{cm}$ and;

a) For $V=10.9\text{m/s}$

All the parameters were previously calculated.

b) For $V=12.5\text{m/s}$

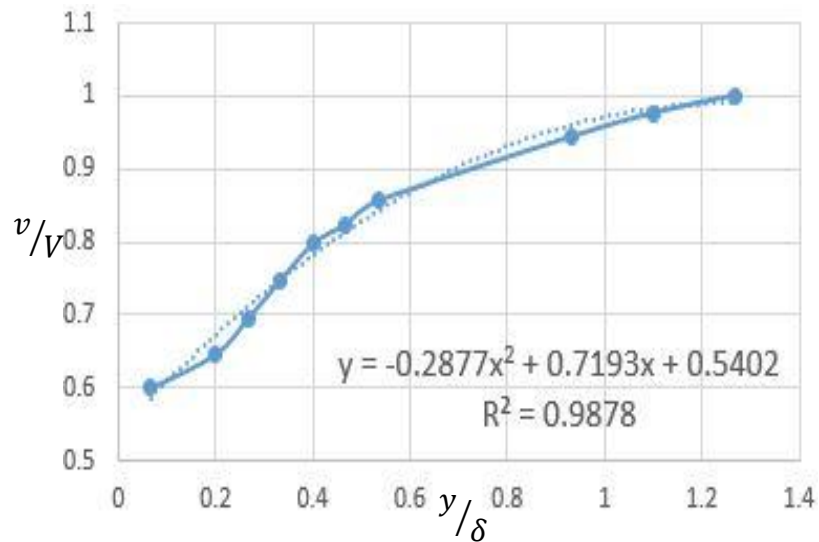


Fig. No. 6.6.1 (e)

$$a = 0.2877, b = 0.7193, c = 0.5402, \delta = 3.0\text{cm}$$

$$\delta^* = 0.5881\text{cm}$$

$$\theta = 0.4249\text{cm}$$

$$\delta_E = 0.594\text{cm}$$

c) For $V=13.6\text{m/s}$

$$a = 0.3659, b = 0.8151, c = 0.5486, \delta = 2.9\text{cm}$$

$$\delta^* = 0.6908\text{cm}$$



RESULTS AND DISCUSSION

$$\theta = 0.4602\text{cm}$$

$$\delta_E = 0.621\text{cm}$$

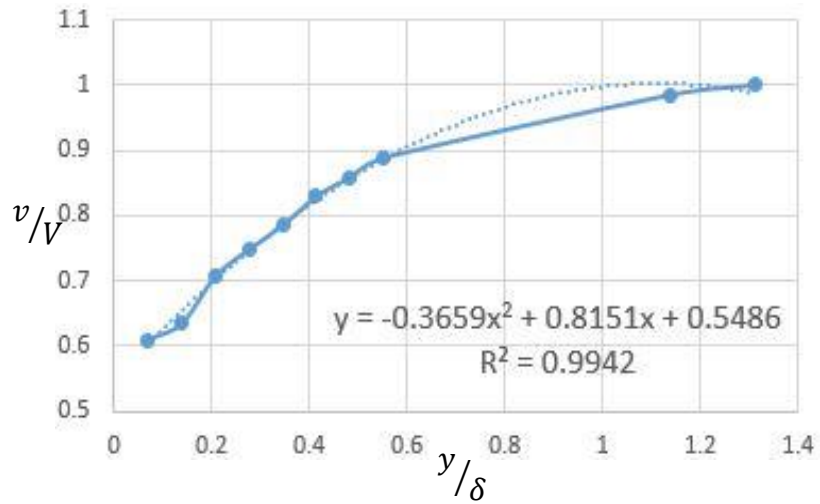


Fig. No. 6.6.1 (f)

3. For $\frac{y}{\delta}$ vs. $\frac{v}{V}$ at $k=375\mu\text{m}$, $V=10.9\text{m/s}$ and;

a) $x=85\text{cm}$

All the parameters were previously calculated.

b) $x=90\text{cm}$

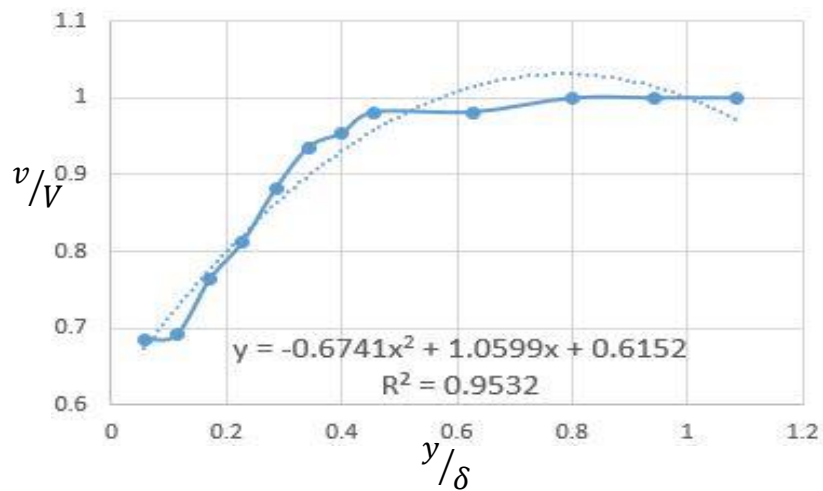


Fig. No. 6.6.1 (g)



RESULTS AND DISCUSSION

$$a = 0.6741, b = 1.0599, c = 0.6152, \delta = 3.5\text{cm}$$

$$\delta^* = 0.2784\text{cm}$$

$$\theta = 0.2040\text{cm}$$

$$\delta_E = 0.354\text{cm}$$

c) $x=95\text{cm}$

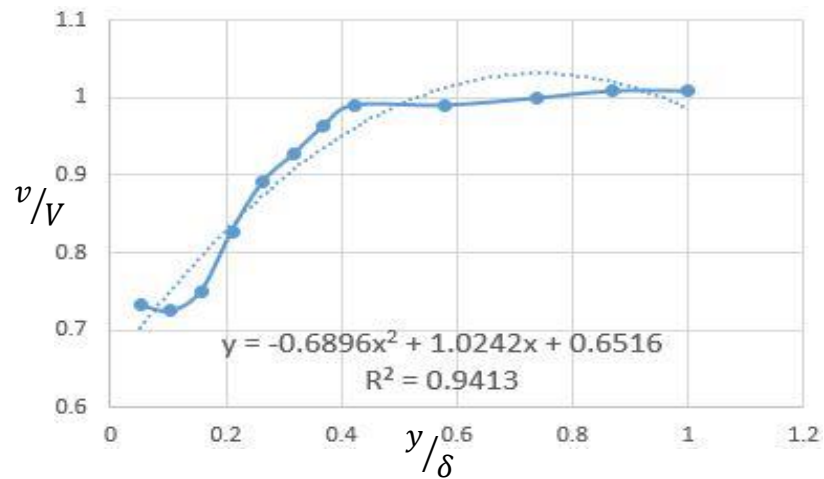


Fig. No. 6.6.1 (h)

$$a = 0.6896, b = 1.0242, c = 0.6516, \delta = 3.8\text{cm}$$

$$\delta^* = 0.2514\text{cm}$$

$$\theta = 0.1893\text{cm}$$

$$\delta_E = 0.336\text{cm}$$

All the above calculated data are tabulated in table no. 7.1(a) for further analysis.



6.7. DISCUSSION

From the above results of the project work, the foremost observation is to be for the velocity profiles. In fig. no. 6.2.1 to 6.2.12 the profiles of velocity explains the theory of boundary layer thickness with respect to roughness of the surfaces. For a particular roughness as we go on increasing the distance from leading edge the B/L thickness tends to increase however for decreasing values of roughness at a particular point the B/L thickness also decreases as compared to the same position for the higher roughness grade. Fig .No. 6.3.1, 6.3.2 and 6.3.3 define the velocity profiles at a particular section and for a particular roughness with different mainstream velocities variations. This represents the effects of roughness and distance from leading edge on mainstream velocities. The variations caused due to the viscous effects at the laminar sub-layer region were clear for the farthest section from the leading edge. As the main stream velocity and Roughness of the surface increases, turbulence also increases. The variations of velocity profile due to changing roughness effects were shown in Fig.no. 6.4.1 and 6.4.2. The turbulence is more due to increase in roughness for a notable distance from leading edge and a given free-stream velocity. However some irregularities were found for the reason that the roughness grades taken, do not possess a significant difference in their roughness height values.

Then the Boundary layer growth in the turbulent region were plotted for varying Roughness profiles at constant mainstream velocity and vice-versa to identify the accuracy of results. Viz. Fig. No. 6.5.1 (a), (b), (c), (d) show the Roughness effects in B/L growth and Fig. No. 6.5.2 (a), (b), (c), (d) define the effects of mainstream velocities. The values of all three boundary layer parameters were calculated by putting the equations obtained

from graphs $\frac{v}{V}$ vs. $\frac{y}{\delta}$ in the theoretical formulae. Typical sample calculations were shown above. Fig.No.6.6.1 (a) to (h) have shown the equations along with the computed values of parameters. A set of values obtained for the given set of one variable and keeping other two variables constant. The values were used for further study and tabulated in favor of developing correlations; Table No. 6.6.1.



RESULTS AND DISCUSSION

Table No.6.6.1 Calculated Values of B/L Parameters with System Variables

Roughness (k), μm	Main-stream Velocity (V), m/s	Distance from leading edge (x), cm	Boundary layer thickness (δ), cm	Displacement thickness (δ^*), cm	Momentum Thickness (θ), cm	Energy Thickness (δ_E), cm
375	10.9	85	3.3	0.34	0.2391	0.6182
345			2.8	0.315	0.2376	0.509
290			2.6	0.307	0.2198	0.4556
125			2.2	0.266	0.1974	0.3395
375	10.9	85	3.3	0.34	0.2376	0.409
	12.5		3	0.5881	0.4249	0.594
	13.6		2.9	0.6908	0.4602	0.621
375	10.9	85	3.3	0.34	0.2376	0.409
		90	3.5	0.2784	0.2040	0.354
		95	3.8	0.2514	0.1893	0.336



7. DEVELOPMENT OF CORRELATION

7.1. GENERAL

The boundary layer parameters are generally most of the help to study the different aspects and responses for flow properties or many more characteristics of a fluid. This project focuses on determination of important boundary layer parameters and their responses towards the turbulent behavior of fluid (air in this case) in the boundary layer zone and development of suitable correlations. For this, experiment data sets are collected by experimentation and certain calculations, as shown in above chapter. So in the present work for establishment of correlations, respective power equations were generated; from which further data were obtained and final correlations with their plots were given. The variables used in this analysis were of two types, i.e. dependent and independent variables. All the variables were processed through the experiments with keeping different roughness, velocity, and distances from leading edge. Then final results were tabulated which give a definite direct formulation for computation of the parameters required under given circumstances.

7.2. DATA PROCESSING

These are the system of variables which are likely to impact the output of the results viz. the free-stream velocity, roughness, distance from leading edge, had been involved in the establishment of the correlations.

DEPENDENT VARIABLES:

Nominal Boundary Layer Thickness = δ ,

Displacement Thickness = δ^* ,

Momentum Thickness = θ ,

Energy Thickness = δ_E ,



CORRELATION & CONCLUSION

INDEPENDENT VARIABLES:

Surface Roughness = k ,

Free/Main Stream Velocity = V ,

Distance from Leading edge = x

Each of the dependent variables can be expressed in terms of the function of all independent variables. They are enumerated as;

$$\delta, \delta^*, \theta, \delta_E = f(k, V, x)$$

$$= C' (k)^{n_1} (V)^{n_2} (x)^{n_3}$$

The exponents n_1, n_2, n_3 correspond to roughness effect (k), main-stream velocity (V), and distance from leading edge (x) respectively. And these exponents can be extracted from the power equations procured by the distinct graphs plotted between each independent variables with each of the dependent ones viz. Fig. No.7.2.1 to Fig.No.7.2.12.

Again these can be expressed for individual dependent parameters as;

$$\delta, \delta^*, \theta, \delta_E = C [(k)^{n_1} (V)^{n_2} (x)^{n_3}]^n$$

The above parameters can be also written separately.

Determination of Exponents for Boundary Layer Thickness-

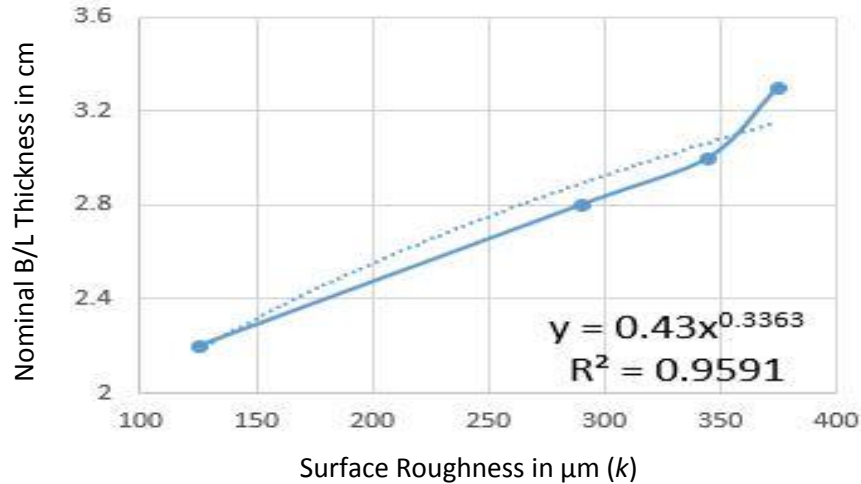


Fig. no. 7.2.1 Determination of n_1 For Nominal/Boundary layer Thickness

Here in Fig.no.7.2.1 the exponent n_1 of surface roughness was obtained from the equation of plots of Roughness (k) vs. Nominal B/L thickness (δ) as follows;

$$\delta = 0.43 k^{0.3363}$$

$$\Rightarrow n_1 = 0.3363$$

Co-efficient of the parameter is to be neglected.

Similarly, the exponent n_2 and n_3 which are the respective powers of ambient velocity and distance from leading edge, were obtained from the equations of plots conceived from free-stream velocity (V) vs. Boundary layer thickness (δ) in Fig. No.7.2.2 and distance from leading edge (x) vs. Boundary layer thickness (δ) respectively in Fig. No.7.2.3. Following the same procedure the corresponding exponents were computed for displacement thickness; viz. Fig. No.7.2.4, 7.2.5, 7.2.6, then for momentum thickness; in Fig. No.7.2.7, 7.2.8, 7.2.9 and for energy thickness as in Fig. No. 7.2.10, 7.2.11, 7.2.12 respectively.

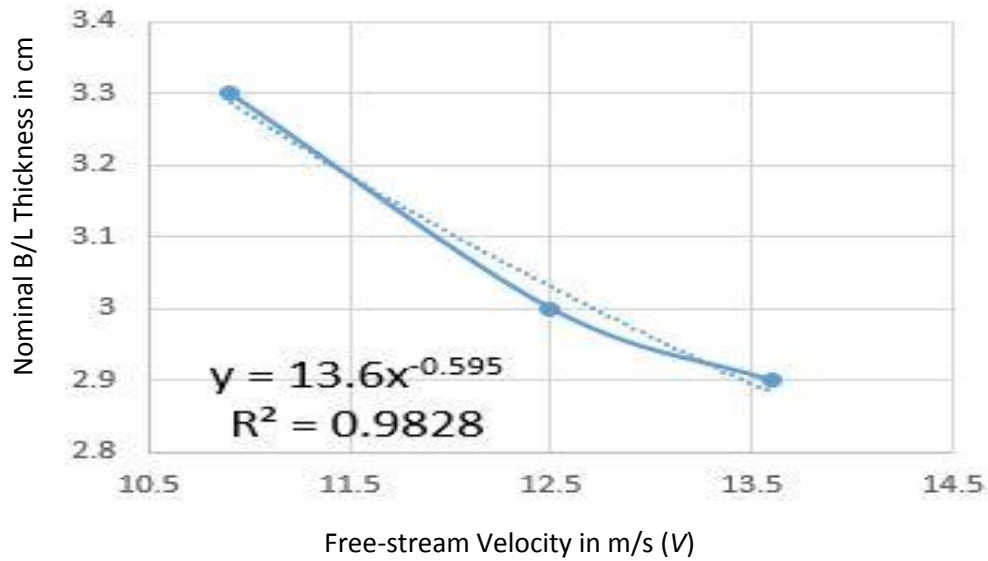


Fig. no. 7.2.2 Determination of n_2 For Nominal/Boundary layer Thickness

$$\Rightarrow n_2 = -0.595$$

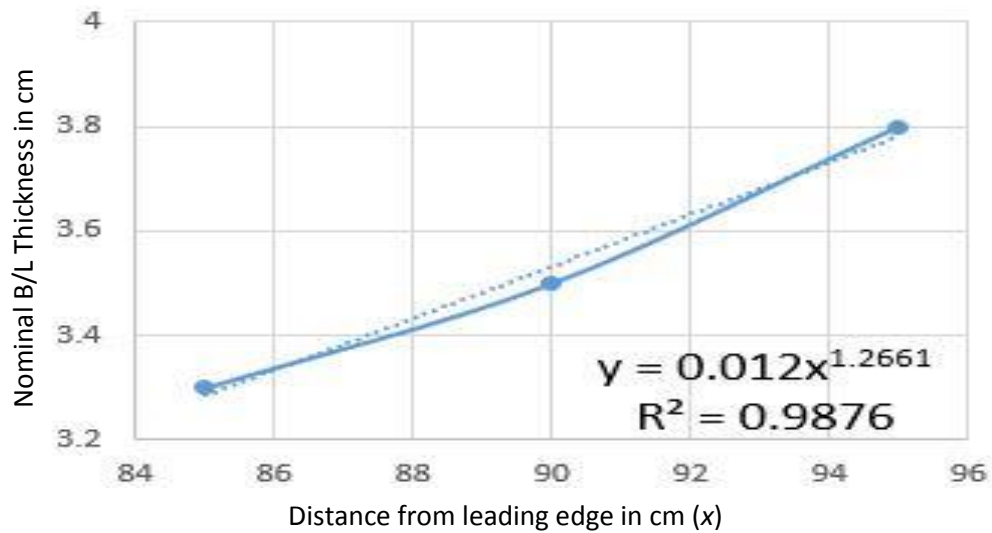


Fig. no. 7.2.3 Determination of n_3 For Nominal/Boundary layer Thickness

$$\Rightarrow n_3 = 1.2661$$

Determination of Exponents for Displacement Thickness-

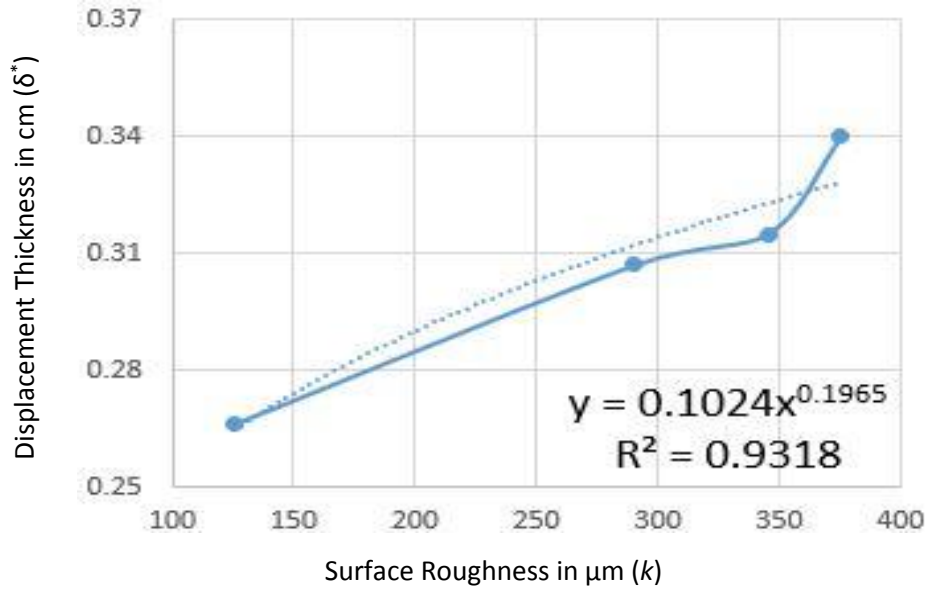


Fig. no. 7.2.4 Determination of n_1 For Displacement Thickness

$$\Rightarrow n_1 = 0.1965$$

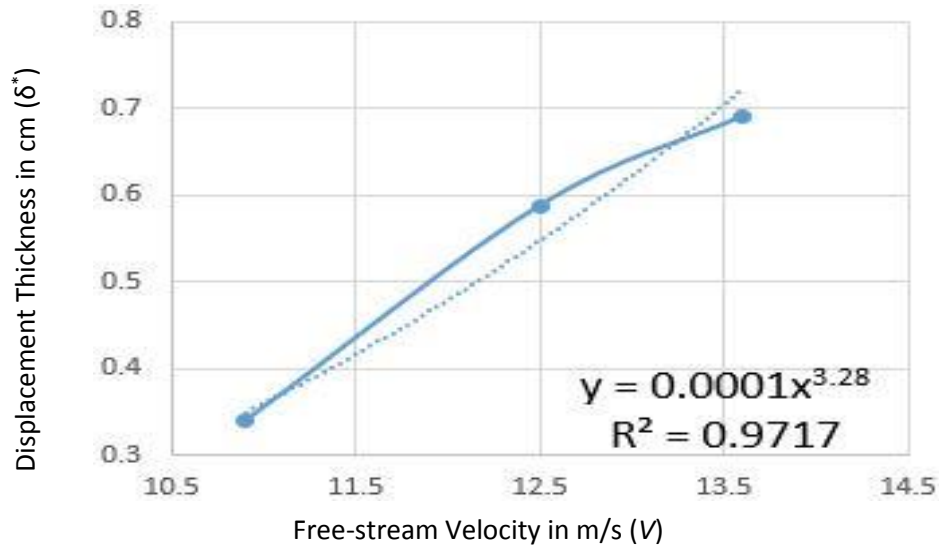


Fig. no. 7.2.5 Determination of n_2 For Displacement Thickness

$$\Rightarrow n_2 = 3.28$$

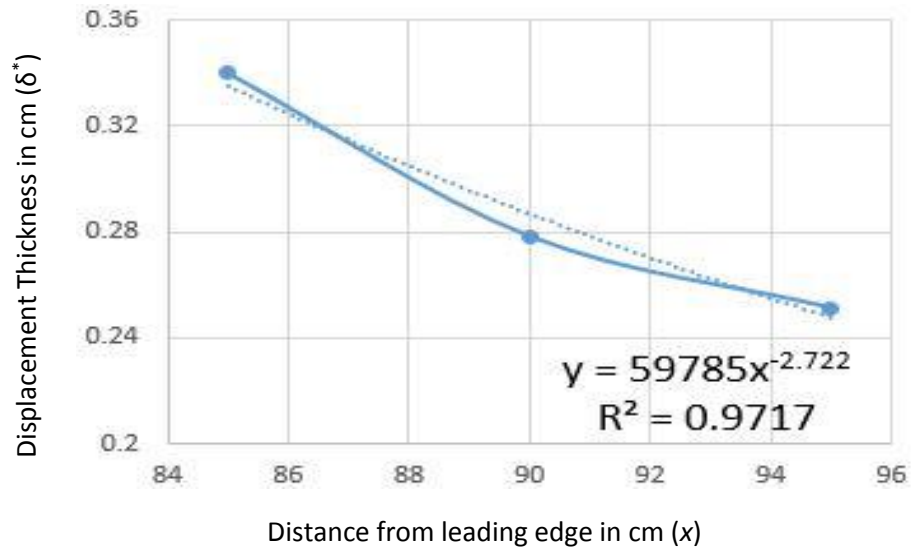


Fig. no. 7.2.6 Determination of n_3 For Displacement Thickness

$$\Rightarrow n_3 = -2.722$$

Determination of Exponents for Momentum Thickness-

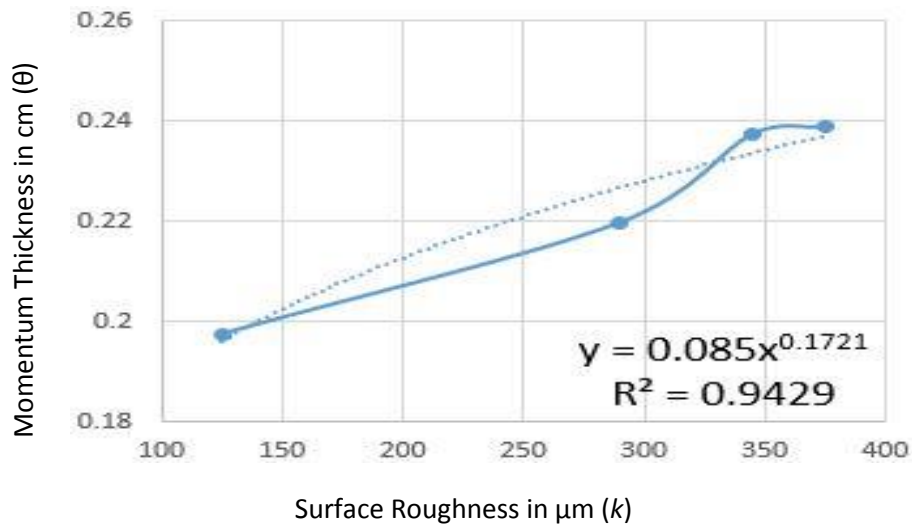


Fig. no. 7.2.7 Determination of n_1 For Momentum Thickness

$$\Rightarrow n_1 = 0.1721$$

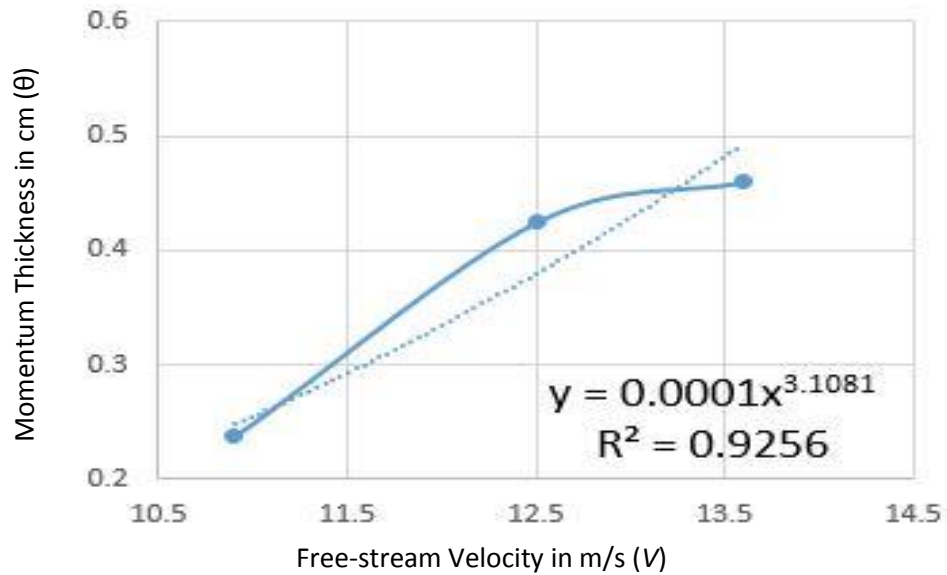


Fig. no. 7.2.8 Determination of n_2 For Momentum Thickness

$$\Rightarrow n_2 = 3.1081$$

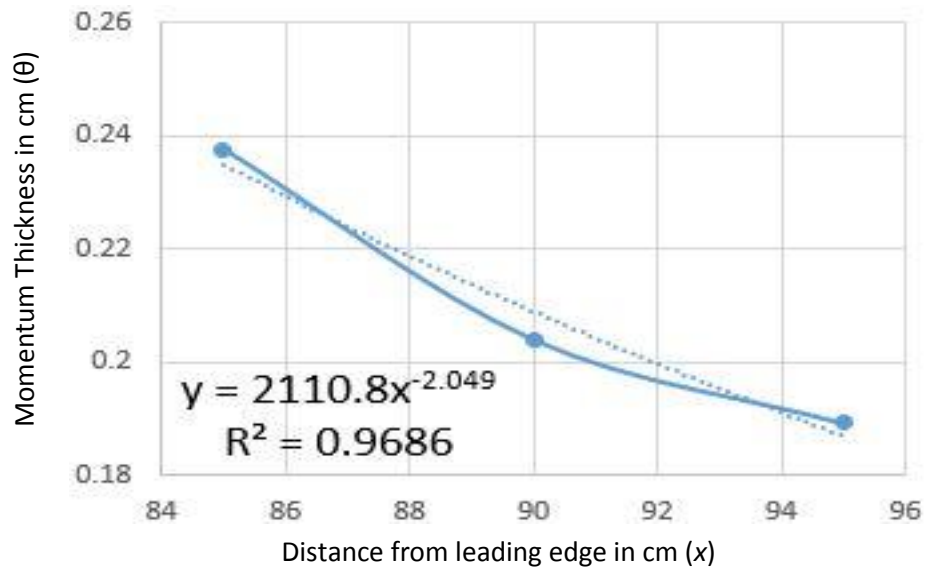


Fig. no. 7.2.9 Determination of n_3 For Momentum Thickness

$$\Rightarrow n_3 = -2.049$$

Determination of Exponents for Energy Thickness-

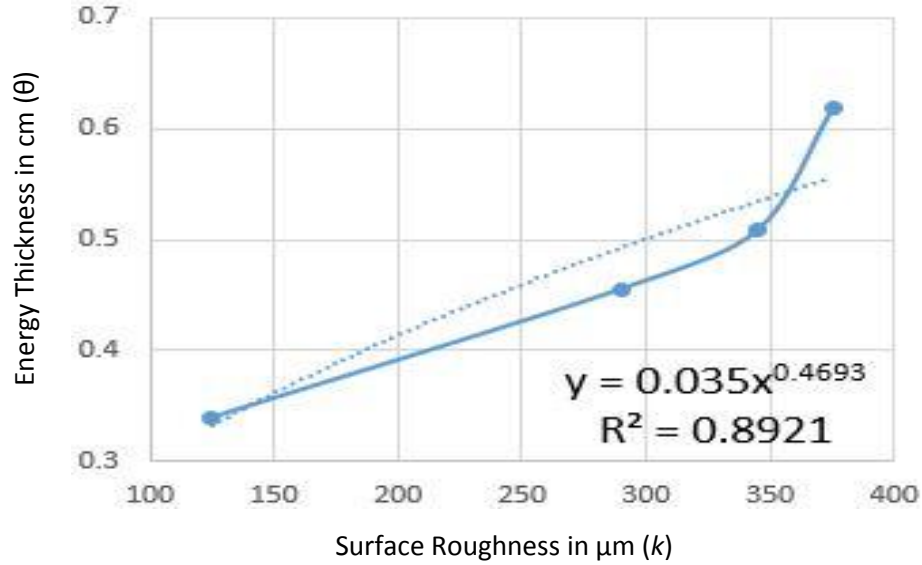


Fig. no. 7.2.10 Determination of n_1 For Energy Thickness

$$\Rightarrow n_1 = 0.4693$$

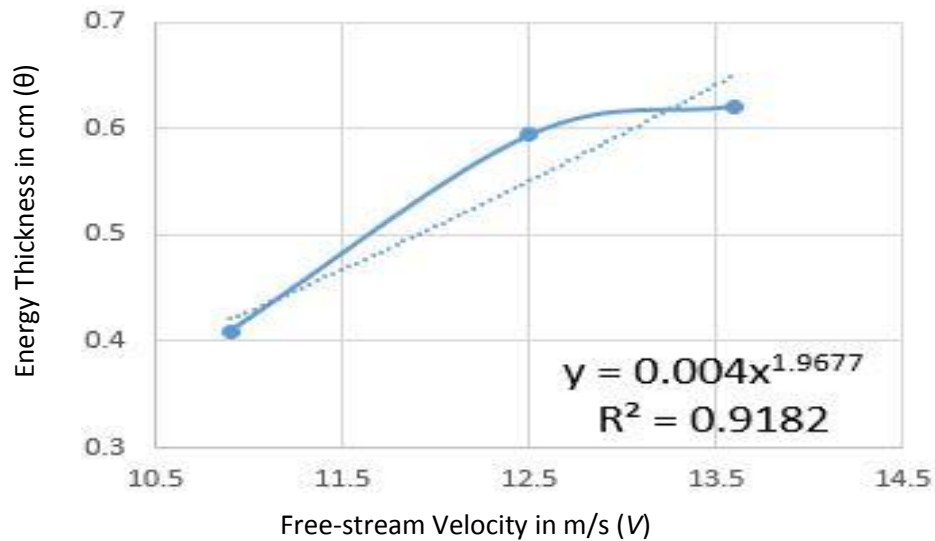


Fig. no. 7.2.11 Determination of n_1 For Energy Thickness

$$\Rightarrow n_2 = 1.9677$$

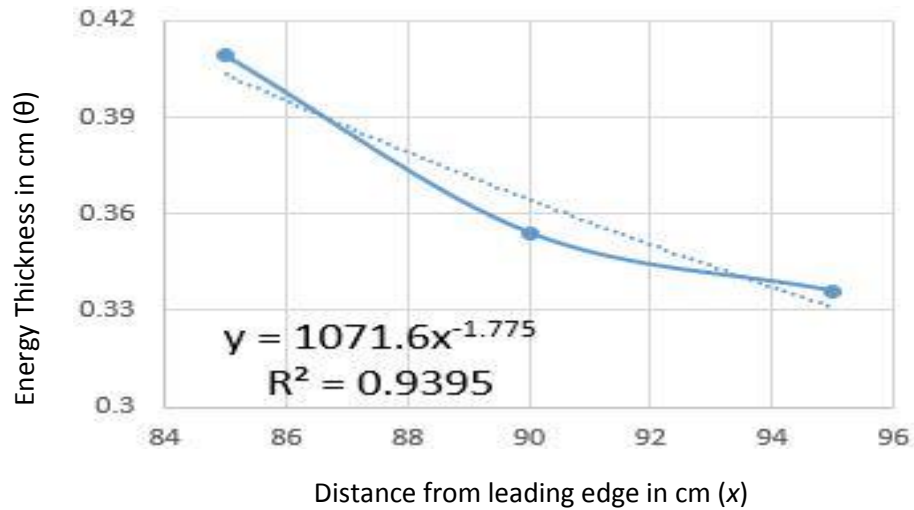


Fig. no. 7.2.12 Determination of n_3 For Energy Thickness

$$\Rightarrow n_3 = -1.775$$

Now From the above sets of graphs (Fig.No. 7.2.1 to 7.2.12) and their corresponding equations, we got the values of the respective exponents for the computation of boundary layer parameters. The values of constant term ‘C’ and the exponent ‘n’ were obtained from the correlation plots between individual dependent variable and the corresponding system parameters, $[(k)^{n_1} (V)^{n_2} (x)^{n_3}]^n$ determined.

These values were tabulated below in Table No. 6.2.1 for the neat and correct presentation of required data and further computation of system parameter (X) and error analysis. When all the calculated values were well arranged in another tabular form, then the plots for final correlations and error were shown in respective figures.

The values in Table No.7.2.1, were used to compute the system parameters so as to plot the graphs for obtaining final equations of correlations viz. Fig.No.7.3.1, 7.3.2, 7.3.3, and



CORRELATION & CONCLUSION

Fig.No.7.3.4. These equations were obtained from the graphs plotted between the corresponding boundary layer parameter and the system parameter $[(k)^{n_1} (V)^{n_2} (x)^{n_3}]$

Table no. 7.2.1. Exponents obtained from Equations

EXPONENTS PARAMETERS	For Roughness (n_1)	For Free-stream velocity (n_2)	For Distance from Leading Edge (n_3)
Boundary Layer Thickness (δ)	0.3363	-0.595	1.2661
Displacement Thickness (δ^*)	0.1965	3.28	-2.722
Momentum Thickness (θ)	0.1721	3.1081	-2.049
Energy Thickness (δ_E)	0.4693	1.9677	-1.775

After obtaining the individual exponents of the effects produced by the variables considered the correct values were put to get the correlations for the separate boundary layer parameter. The values of constant term 'C' and the exponent 'n' were obtained from the correlation plots (Fig. No. 7.3.1, 7.3.2, 7.3.3 and 7.3.4) plotted between individual dependent variable and the corresponding system parameters.

7.3. CORRELATION PLOTS FOR ALL THE BOUNDARY LAYER PARAMETERS

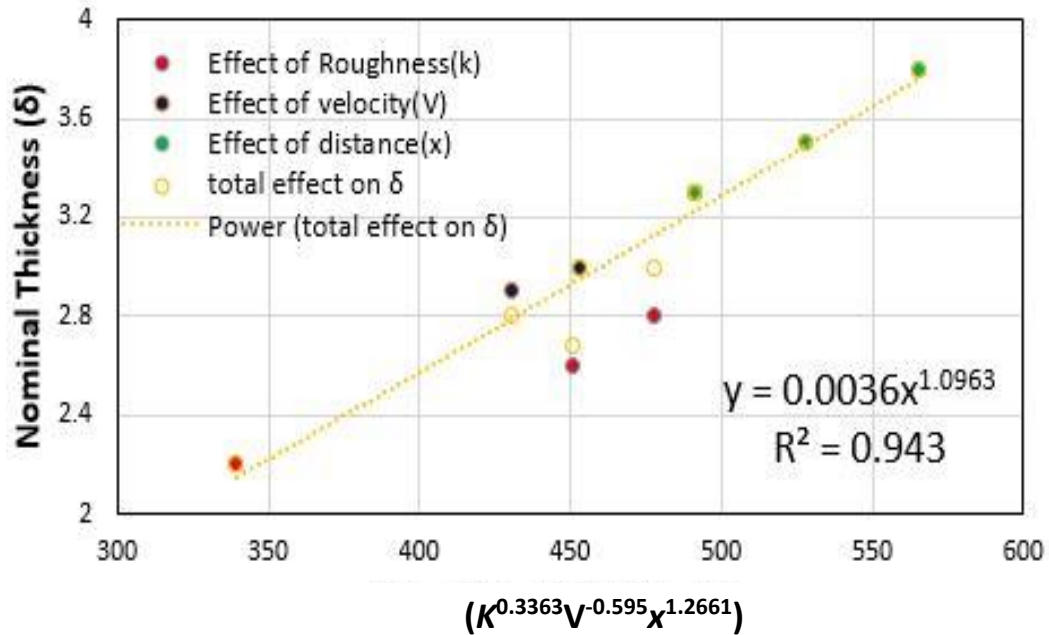


Fig. no. 7.3.1 Correlation Plot of Nominal Thickness with System Variable

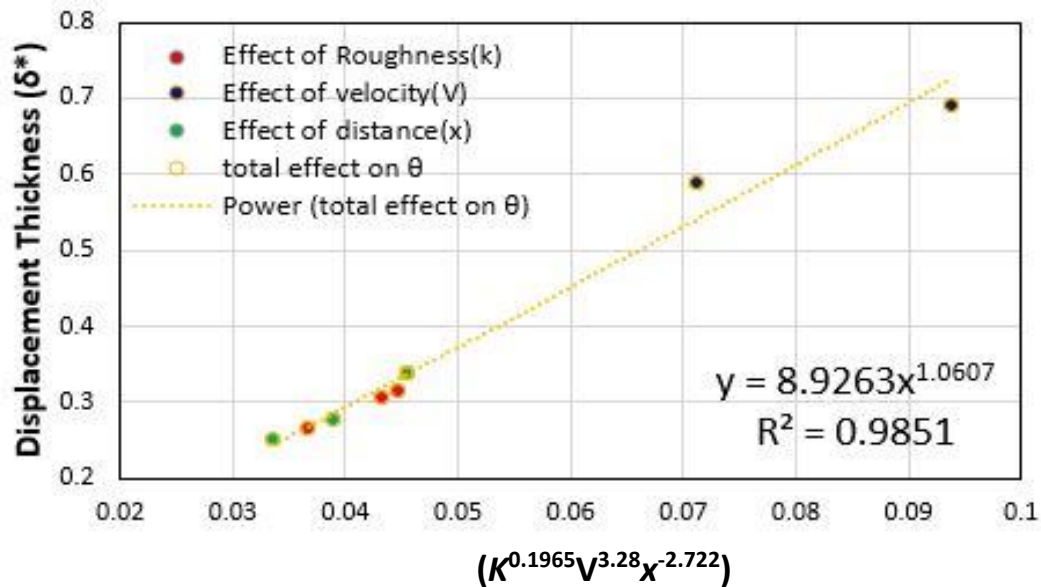


Fig. no. 7.3.2 Correlation Plot of Displacement Thickness with System Variable



Table no.7.3.1. Comparison of Experimental and Predicted values of Nominal B/L Thickness using Developed Correlation

Roughness (k), μm	Main-stream Velocity (V), m/s	Distance from leading Edge (x), cm	Values of Nominal B/L Thickness, (δ) cm		%Error
			Experimental δ	Predicted δ	
375	10.9	85	3.3	3.211306663	-2.6877
345			2.8	3.114087925	11.2174
290			2.6	2.920950459	12.3442
125			2.2	2.141775771	-2.6465
375	10.9	85	3.3	3.211306663	-2.6877
	12.5		3	2.936843287	-2.1052
	13.6		2.9	2.779635177	-4.1505
375	10.9	85	3.3	3.211306663	-2.6877
		90	3.5	3.476462474	-0.6725
		95	3.8	3.747398719	-1.3842

From the above comparison Table no.8.3.1 following mean and standard deviation for boundary layer thickness were found for the set of experimental and predicted values.

$$\text{Mean } (X_{av}) = 0.453960$$

$$\text{Standard deviation } (\sigma) = 6.044763$$



CORRELATION & CONCLUSION

Table No.7.3.2. Comparison of Experimental and Predicted values of Displacement Thickness using Developed Correlation

Roughness in μm (k)	Main-stream Velocity in m/s (V)	Distance from leading Edge in cm (x)	Values of Displacement Thickness (δ^*), cm		%Error
			Experimental δ^*	Predicted δ^*	
375	10.9	85	0.34	0.335590424	-1.3003
345			0.315	0.329808576	4.6976
290			0.307	0.318084210	3.6070
125			0.266	0.266909693	0.3386
375	10.9	85	0.34	0.335590424	-1.3002
	12.5		0.5881	0.540453606	-8.1048
	13.6		0.6908	0.724759409	4.9124
375	10.9	85	0.34	0.335590424	-1.3003
		90	0.2784	0.284536692	2.2008
		95	0.2514	0.243412603	-3.1804

From the above comparison Table no.8.3.2 following mean and standard deviation for displacement thickness were found for the set of experimental and predicted values.

$$\text{Mean } (X_{av}) = 0.05705$$

$$\text{Standard deviation } (\sigma) = 4.01402$$

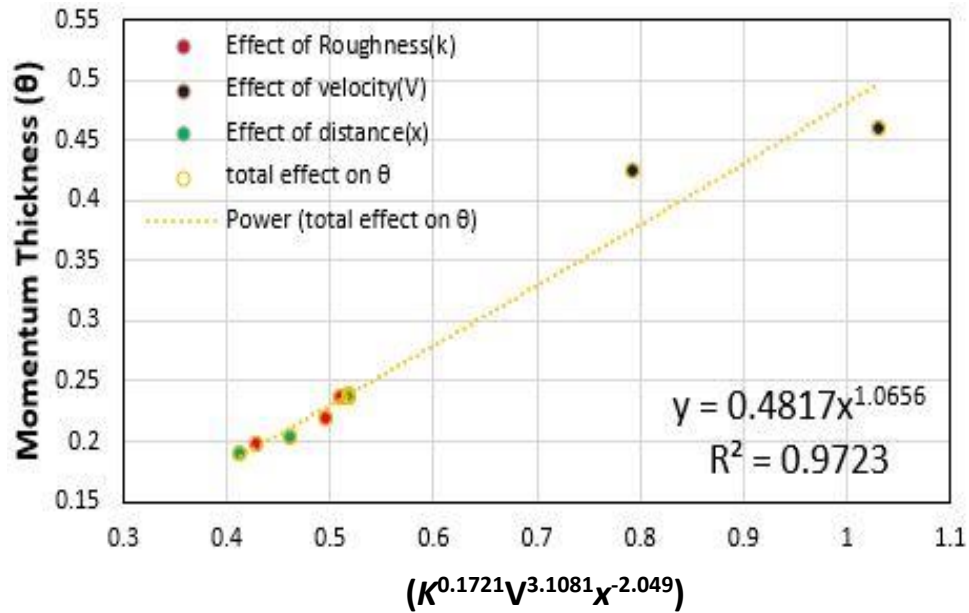


Fig. no. 7.3.3 Correlation Plot of Momentum Thickness with System Variable

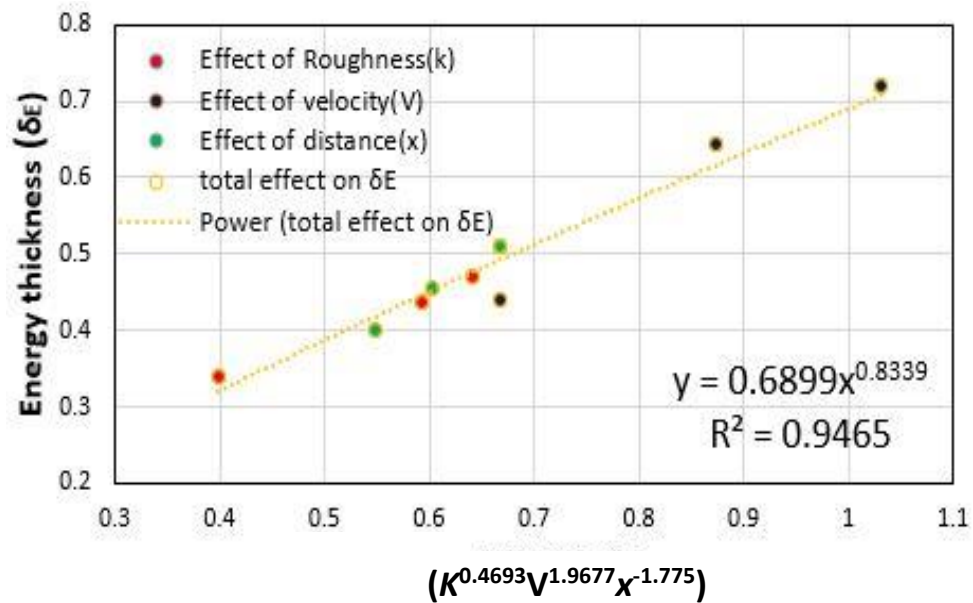


Fig. no. 7.3.4 Correlation Plot of Energy Thickness with System Variable



CORRELATION & CONCLUSION

Table No.7.3.3. Comparison of Experimental and Predicted values of Momentum

Thickness using Developed Correlation

Roughness in μm (k)	Main-stream Velocity in m/s (V)	Distance from leading Edge in cm (x)	Values of Momentum Thickness, (θ) cm		%Error
			Experimental θ	Predicted θ	
375	10.9	85	0.2391	0.238810905	-0.1209
345			0.2376	0.235186946	-1.0156
290			0.2198	0.227814706	3.6464
125			0.1974	0.195233798	-1.0974
375	10.9	85	0.2376	0.238810905	0.5096
	12.5		0.4249	0.375891965	-11.5340
	13.6		0.4602	0.497024306	8.0018
375	10.9	85	0.2376	0.238810905	0.5096
		90	0.20403	0.210791932	3.3142
		95	0.1893	0.187320376	-1.0458

From the above comparison Table no.8.3.3, the following mean and standard deviation for momentum thickness were found for the set of experimental and predicted values.

$$\text{Mean } (X_{av}) = 0.116798$$

$$\text{Standard deviation } (\sigma) = 5.00076$$



CORRELATION & CONCLUSION

Table No.7.3.4. Comparison of Experimental and Predicted values of Energy Thickness using Developed Correlation

Roughness in μm (k)	Main-stream Velocity in m/s (V)	Distance from leading Edge in cm (x)	Values of Energy Thickness, (δ_E) cm		%Error
			Experimental δ_E	Predicted δ_E	
375	10.9	85	0.492646	0.5092	0.4835
345			0.476830	0.4709	4.1557
290			0.445500	0.4363	5.0293
125			0.320490	0.3395	-2.8992
375	10.9	85	0.492646	0.439	15.4300
	12.5		0.616793	0.644	-1.3256
	13.6		0.708341	0.721	1.3189
375	10.9	85	0.492646	0.509	-0.4444
		90	0.452681	0.454	2.5615
		95	0.417865	0.402	6.9198

From the above comparison Table no.8.3.4 following mean and standard deviation for energy thickness were found for the set of experimental and predicted values.

$$\text{Mean } (X_{av}) = 3.026262$$

$$\text{Standard deviation } (\sigma) = 5.331748$$



7.4. CORRELATIONS ESTABLISHMENT

From *Fig.No. 7.3.1*, the correlation was obtained from the Nominal B/L thickness vs.

$[(k)^{n_1} (V)^{n_2} (x)^{n_3}]$ graph, for nominal B/L thickness along with regression coefficient (R^2)

to define the accuracy. Now the correlations were obtained as follows,

$$\delta = 0.0036[k^{n_1}V^{n_2}x^{n_3}]^{1.0963}$$

Here $n_1 = 0.3363$, $n_2 = -0.595$, $n_3 = 1.2661$ and $R^2 = 0.943$

From *Fig.No. 7.3.2*, the correlation was obtained from the displacement thickness vs.

$[(k)^{n_1} (V)^{n_2} (x)^{n_3}]$ graph, for displacement thickness;

$$\delta^* = 8.9263[k^{n_1}V^{n_2}x^{n_3}]^{1.0607}$$

Here $n_1 = 0.1965$, $n_2 = 3.28$, $n_3 = -2.722$ and $R^2 = 0.985$

From *Fig.No. 7.3.3*, the correlation was obtained from the Momentum thickness vs.

$[(k)^{n_1} (V)^{n_2} (x)^{n_3}]$ graph, for momentum thickness;

$$\theta = 0.4817[k^{n_1}V^{n_2}x^{n_3}]^{1.0656}$$

Here $n_1 = 0.0.1721$, $n_2 = 3.1081$, $n_3 = -2.049$ and $R^2 = 0.972$

From *Fig.No. 7.3.1*, the correlation was obtained from the Energy thickness vs.

$[(k)^{n_1} (V)^{n_2} (x)^{n_3}]$ graph, for energy thickness;

$$\delta_E = 0.6899[k^{n_1}V^{n_2}x^{n_3}]^{0.8339}$$

Here $n_1 = 0.4693$, $n_2 = 1.9677$, $n_3 = -1.775$ and $R^2 = 0.946$

7.5. COMPARISON GRAPHS OF BOUNDARY LAYER PARAMETERS

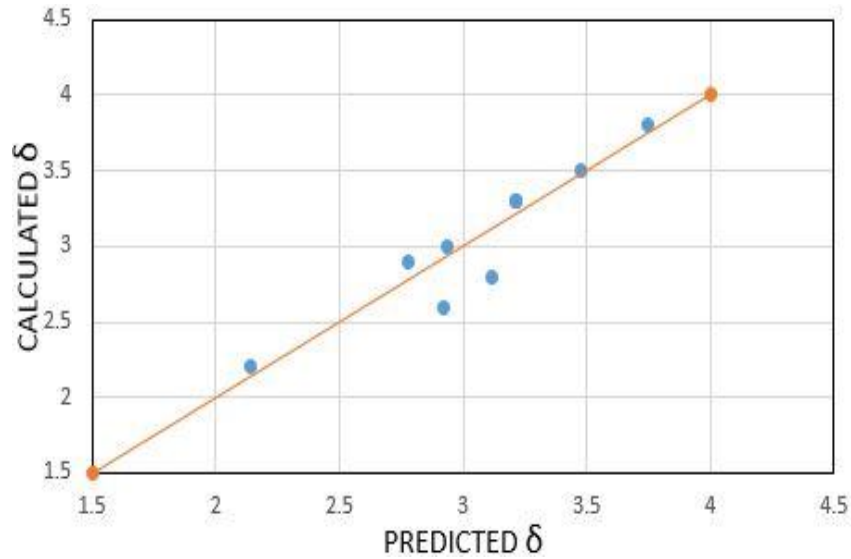


Fig. no. 7.4.1 Comparison between experimental and predicted values of Nominal B/L Thickness (δ)

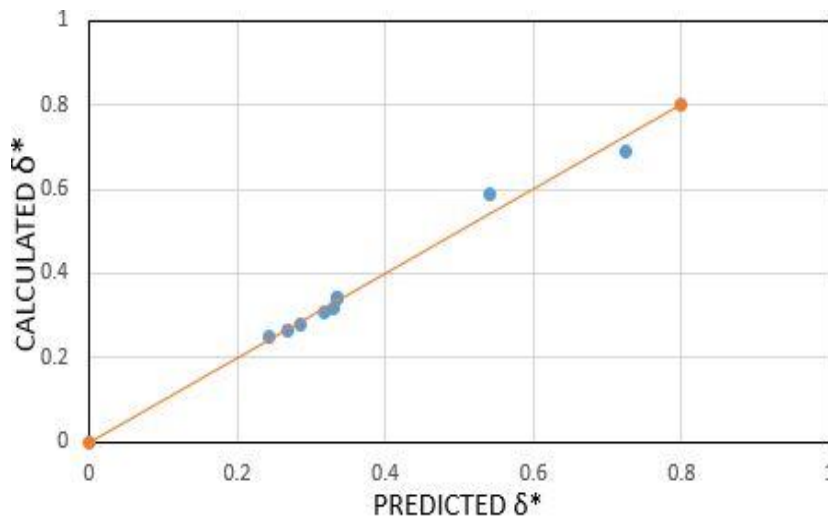


Fig. no. 7.4.2 Comparison between experimental and predicted values of Displacement Thickness (δ^*)

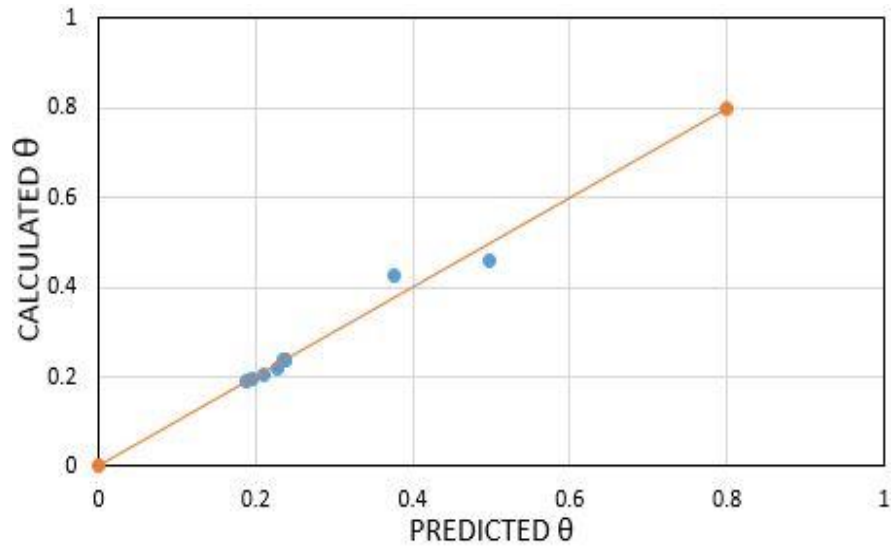


Fig. no. 7.4.3 Comparison between experimental and predicted values of Momentum Thickness (θ)

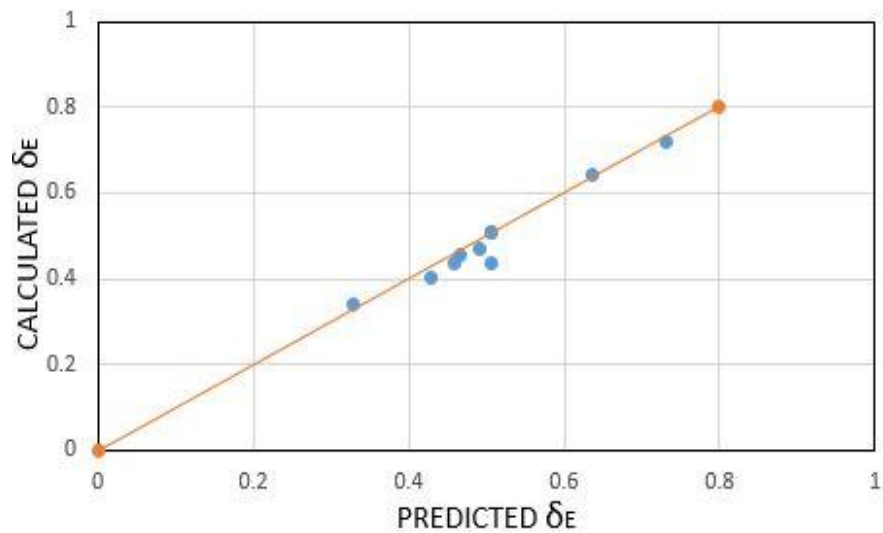


Fig. no. 7.4.4 Comparison between experimental and predicted values of Energy Thickness (δ_E)

The correlations obtained were tabulated for comparison with experimental results and error checking purposes. Also, the mean and standard deviation values of B/L thickness,



CORRELATION & CONCLUSION

displacement thickness, momentum thickness and energy thickness were shown in Table No. 7.3.1, 7.3.2, 7.3.3 and 7.3.4 respectively. At last but not the least table no. 7.4 shows the effect of a specific variable while other two variables are kept constant.

7.6. CONCLUSIONS

From the extensive experimentation and data analysis, the following conclusions have been made:

- 1) The surface roughness, main stream velocity on the position from the leading edge have significance effects on velocity profile, boundary layer growth, nominal boundary layer thickness, displacement thickness, momentum thickness and the energy thickness.
- 2) the boundary layer thickness increases as the distance from the leading edge (turbulent zone) increases.
- 3) At a fixed position position from the leading edge (x) and fixed vertical distance from the surface (y), and for a given surface roughness, the velocity increases with increase in main stream velocity.
- 4) For a given distance from the leading edge and at constant mainstream velocity, the velocity has also been found to decrease with increase in roughness of the surface. However little disturbances are possible if there is not a large difference between the roughness values.
- 5) The boundary layer thickness increase with increase in roughness and also with increase in distance from leading edge.



CORRELATION & CONCLUSION

- 6) The B/L thickness, displacement thickness, momentum thickness and energy thickness increase with increase in surface roughness. While for increase of mainstream velocity all the parameters increase except B/L thickness. At last but not the least all the parameters decrease with increasing distance from leading edge except for B/L thickness.

7.7. SCOPE FOR FUTURE WORK

As we know that turbulence is a phenomenon involved in our day to day life, for which it is required to study the fetures and its behavior towards the structures, objects, automobiles etc. from engineering point of view. The scope for this project relies on the theory that boundary layer exists wide over everywhere in this world so considering turbulence, an essential part one can determine the parameters within permissible limits for safe design purpose of structures or any construction and many other fields like industries. The importance of this project for water resource engineering fields specifically involves the study of Hydraulic structures which are continuously comes under the influence of atmospheric boundary layer; so that many features like durability of the structure, design parameters can be enhanced for the safe and better withstanding of the structures. Further studies to obtain correlations on velocity, can be done as a scope of the future work.



REFERENCES

- 1) **K. V. S. Namboodiri and Dileep Puthillam Krishnan, (2014)**, “Coastal Boundary Layer Characteristics of Wind, Turbulence, and Surface Roughness Parameter over the Thumba Equatorial Rocket Launching Station, India”, *Journal of Climatology*, vol. 2014, Article ID 504178, 21 pages, 2014. doi:10.1155/2014/504178,
- 2) **J. Cardillo and Yi Chen, (2013)**, “DNS of a turbulent boundary layer with surface roughness” *Journal of Fluid Mechanics*, Volume 729, August 2013, pp- 603- 637 ©2013 Cambridge University Press, doi: <http://dx.doi.org/10.1017/jfm.2013.326>,
- 3) **Hedenstrom and Anders, (2009)**, "High-speed stereo DPIV measurement of wakes of two bat species flying freely in a wind tunnel." *Experiments in Fluids* 46.5 2009: 923-932, doi 10.1007/s00348-009-0634-5,
- 4) **Cheryl Klipp, (2007)**, "Wind direction dependence of atmospheric boundary layer turbulence parameters in the urban roughness sub layer." *Journal of Applied Meteorology and Climatology* 46.12,2007:2086-2097, doi: <http://dx.doi.org/10.1175/2006JAMC1298.1>.
- 5) **B. Massey and J. Ward-Smith, (2006)** "*Mechanics of Fluids*", Taylor and Francis, 8th Edition, 2006.
- 6) **Tetsuro Tamura, (2006)**, "Experimental study on roughness effects on turbulent boundary layer flow over a two-dimensional steep hill." *Journal of wind*



REFERENCES & PUBLICATIONS

- engineering and industrial aerodynamics*, Volume 94, Issue 1, January 2006, pp-1–19, 94.1, doi:10.1016/j.jweia.2005.10.001,
- 7) **James Benson (2005)**, “Boundary-layer response to a change in surface roughness”, Department of Meteorology, *The University of Reading*, MSc. Thesis
 - 8) **Aubertine and Carolyn D, (2004)**, "Parameters controlling roughness effects in a separating boundary layer." *International journal of heat and fluid flow*", Volume 25, Issue 3, June 2004, Pages 444–450. doi:10.1016/j.ijheatfluidflow.2004.02.007
 - 9) **F.M. White, (2003)**, "Fluid Mechanics", *McGraw-Hill, 5th Edition*.
 - 10) **B.R. Munson, (2002)**, "Fundamentals of Fluid Mechanics", *John Wiley, 4th Edition*.
 - 11) **R. A. Antonia, (1999)**, “Surface roughness effects in turbulent boundary layers” *Experiments in Fluids 27*, ©Springer-Verlag, 1999: Pg.No.450-460.
 - 12) **Blom and L. Wartena, (1969)**, "The influence of changes in surface roughness on the development of the turbulent boundary layer in the lower layers of the atmosphere." *Journal of the Atmospheric Sciences 26*: 255-265.

PUBLICATIONS FROM THE WORK

- 1) **A. Singh and A. Kumar, (2015)**, “Effect of mainstream air velocity on velocity profile over a rough flat surface. *International Journal of Computational Engineering Research (IJCER)*, Vol.05 (Issue-02), p.16-19, February, 2015.
- 2) **A. Singh, A. Kumar and M. Mallick (2015)**, “Effect of main stream velocity and roughness on velocity profile on Flat Surface in Turbulent Boundary Layer Zone”. *IOSR Journal of Mechanical and Civil Engineering*, Issue X, p.23-26, April, 2015.